PERFORMANCE MEASUREMENT
OF A TEN KILOWATT
HORIZONTAL AXIS WIND TURBINE

by

Thomas E. Benim

Thesis submitted to the Graduate Faculty of the
Virginia Polytechnic Institute and State University
in partial fulfillment of the requirements for the degree of
MASTER OF SCIENCE
in
Mechanical Engineering

APPROVED:

W. F. O'Brien, Jr.

H. L. Moses

H. L. Wood

September, 1977

Blacksburg, Virginia

II. ACKNOWLEDGMENTS

The author wishes to thank the members of his advisory committee: Professors H. L. Moses, W. F. O'Brien, Jr., Chairman, and H. L. Wood. The continued assistance of Dr. O'Brien is particularly acknowledged.

The work of all the members of the VPI&SU Wind-Powered Apple Cooling & Storage Research project is acknowledged.

The support of the USDA, Agricultural Research Service, is recognized.

The author thanks his wife, , for her encouragement and moral support.

III. TABLE OF CONTENTS

IV. LIST OF FIGURES

Appendix Figures

V. LIST OF TABLES

APPENDIX TABLES

VI. NOMENCLATURE

A	Area
a	Axial Interference Factor
B_{max}	Maximum Thickness of Blade Section
C	Chord Length
C_p	Power Coefficient
D	Distance from LE to B_{max}
E	Kinetic Energy
f	Frequency
I	Current
L	Length
L'	Lift Vector
L/D	Lift/Drag
LE	Leading Edge Thickness
m	Mass
P	Power
P_∞	Total Power of Wind at V_∞
R	Rotor Radius
r	Blade Element Radius
t	Time
TE	Trailing Edge Thickness
u	Wind Speed at Rotor Plane
u_1	Final Wind Speed
V_∞	Free Stream Velocity
W	Measurement Uncertainty

W'	Relative Wind Velocity
X	Tip Speed Ratio
α	Angle of Attack
ρ	Density
σ	Standard Deviation
θ	Blade Pitch
Ω	Angular Velocity

VII. INTRODUCTION

Wind has been used for centuries to propel boats, pump water, and, more recently, as a source of electrical power. The use of wind turbines to generate electricity has been limited to remote areas because of the availability of cheap, reliable electrical power in most developed countries. The dwindling supply and increased cost of fossil fuels, coupled with the unfulfilled dreams of unlimited nuclear power have prompted increased interest in all types of wind turbine generators.

Work is currently underway at Virginia Polytechnic Institute and State University (VPI&SU) to build a wind-powered, refrigerated, apple storage facility. This project, sponsored by the Agriculture Research Service, United States Department of Agriculture, is a feasibility project to study the merits of wind power for apple storage applications.

Since the purpose of this project is to apply wind power to a specific use, a commercially available windmill was purchased, so that design efforts could be concentrated on the energy storage and refrigeration systems. After initial design considerations and wind velocity surveys, it was decided to purchase an Electro[1] WVG-120G wind generator which has a peak output of 10 kW. [1][2]

---

[1] Electro, G.m.b.H. Winterhur, Switzerland.

[2] Numbers in brackets refer to references listed in LITERATURE CITED.

Data concerning the performance of the wind generator were incomplete and tended to be stated in general terms. Specific performance data are essential to the evaluation of the overall project's success. This thesis is concerned with the development of the windmill testing facilities at VPI&SU and the initial performance testing of the Electro WVG-120G wind generator.

VIII. REVIEW OF LITERATURE

Overview

Although wind turbines have been used for centuries, the modern development of wind turbines (particularly for the generation of electricity) began at the close of World War I. According to Putnam [2], early investigators studied three types of wind turbines: The spinning cylinder (Magnus effect), the Savonius rotor, and the propeller type. Modern literature divides windmills into two broad categories designated by the orientation of the rotor axis to the ground, i.e. vertical axis or horizontal axis. Some researchers refer to vertical axis wind turbines as crosswind-axis machines and horizontal axis turbines as wind-axis machines.

The two most popular vertical axis rotors are the Darrieus rotor and the Savonius rotor. The Darrieus rotor is somewhat more economical to build in terms of material used, but the Savonius rotor is popular with individual experimenters due to the ease of construction using readily available materials. The advantages of vertical axis wind turbines are two. First, they are sensitive to winds from any direction and can respond to gusts without being oriented to the direction of flow. Second, the generator can be located at the base, reducing structural loads.

A large Darrieus wind turbine 19 m (62 ft) high and 17 m (56 ft) in diameter is currently being tested at Sandia Laboratories. The

wind turbine is expected to produce 60 kW in a 12.5 m/s (28 mile/h) wind [3].

Two common examples of horizontal axis wind turbines are the American farm windmill and the Dutch windmills. Both of these produce high torque at a low rotational speed making them ideal for driving pumps and other machinery. To drive an electrical generator a 2- or 3-bladed, high speed wind turbine is more effective since less gearing is required. High speed wind turbines also are able to extract more of the wind energy. Figure 1 shows performance characteristics vs. tip speed ratio for several types of wind turbines.

Many large-scale horizontal axis wind turbines have been built as test units. The largest was the Smith - Putnam wind turbine, built in Vermont during World War II [2]. The machine had a capacity of 1.25 MW and was operated more than 1100 hours before a blade failure caused cancellation of the program. The notoriety of this turbine lies not with its material failure but with its success at proving that a large wind turbine can be interfaced to a commercial utility network.

Large horizontal axis wind turbines have been constructed with the rotor plane upwind and downwind of the tower [4]. The downwind orientation provides an improved safety margin since the blades can flex in a strong wind without hitting the tower. However, the wake of the tower can induce periodic stresses in the blades, which may cause premature failure. This problem is being studied at Sandusky, Ohio by NASA engineers of the Lewis Research Center.

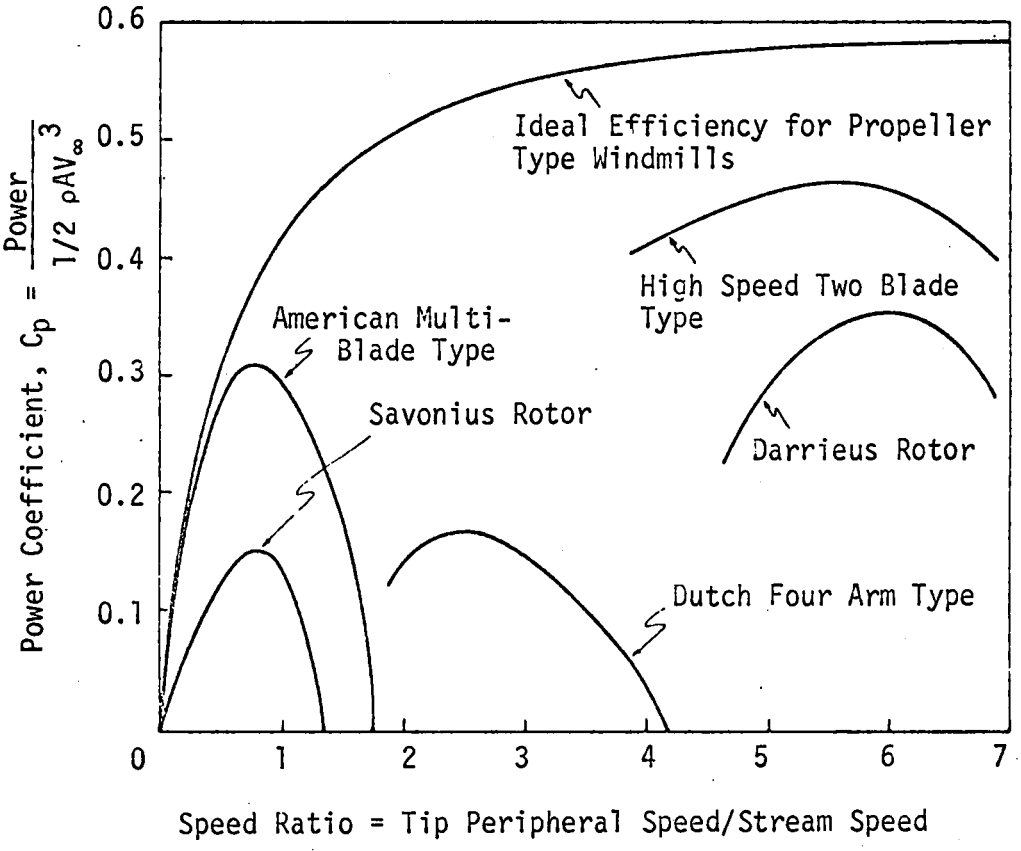

Figure 1. Typical Performance of Wind Power Machines. (From Reference 8)

While development efforts of large wind turbines command most of the current attention, the largest commercially available wind turbine is rated at approximately 10 kW output. The need for small wind energy systems, particularly for agricultural use, has been pointed out by Rueth [5] and Liljedahl [6].

Wilson [7] points out the need for research on production windmills, citing the fact that no performance data are available except some rather limited figures from manufacturers. In addition to performance, cost and reliability of commercial units must be improved.

Wind Energy Aerodynamics

Fundamental windmill aerodynamic theory has been developed from one dimensional momentum theory. The basic ideas of this theory are outlined below.

The kinetic energy of an airstream of mass, m, and velocity, V_∞, is

$$E = \frac{1}{2} m V_\infty^2 \tag{1}$$

If ρ is the density, A is the cross-sectional area of the airstream, and L is a reference length, then

$$E = \frac{1}{2} \rho A L V_\infty^2 \tag{2}$$

But L can be expressed as

$$L = V_\infty t \tag{3}$$

Since power is the time rate of change of energy, using Equations (2) and (3),

$$P_\infty = \frac{dE}{dt} = \frac{1}{2}\rho A V_\infty^3 \tag{4}$$

Following the axial momentum approach of Wilson and Lissaman [8] and referring to Fig. 2,

$$u = \frac{V_\infty + u_1}{2} \tag{5}$$

The power extracted from the airstream is given by

$$P = \frac{\rho A u}{2}(V_\infty + u_1)(V_\infty - u_1) \tag{6}$$

If we define an axial interference factor (a), so that

$$V_\infty - u = a\, V_\infty \tag{7}$$

and

$$V_\infty - u_1 = 2a\, V_\infty \tag{8}$$

Power can be expressed as

$$P = \frac{1}{2}\rho\, A V_\infty^3 [4\, a(1 - a)^2] \tag{9}$$

A power coefficient, C_p, can now be defined as

$$C_p \equiv \frac{P}{P_\infty} \tag{10}$$

Thus,

$$C_p = \frac{P}{\frac{1}{2}\rho A V_\infty^3} = 4a(1 - a)^2 \tag{11}$$

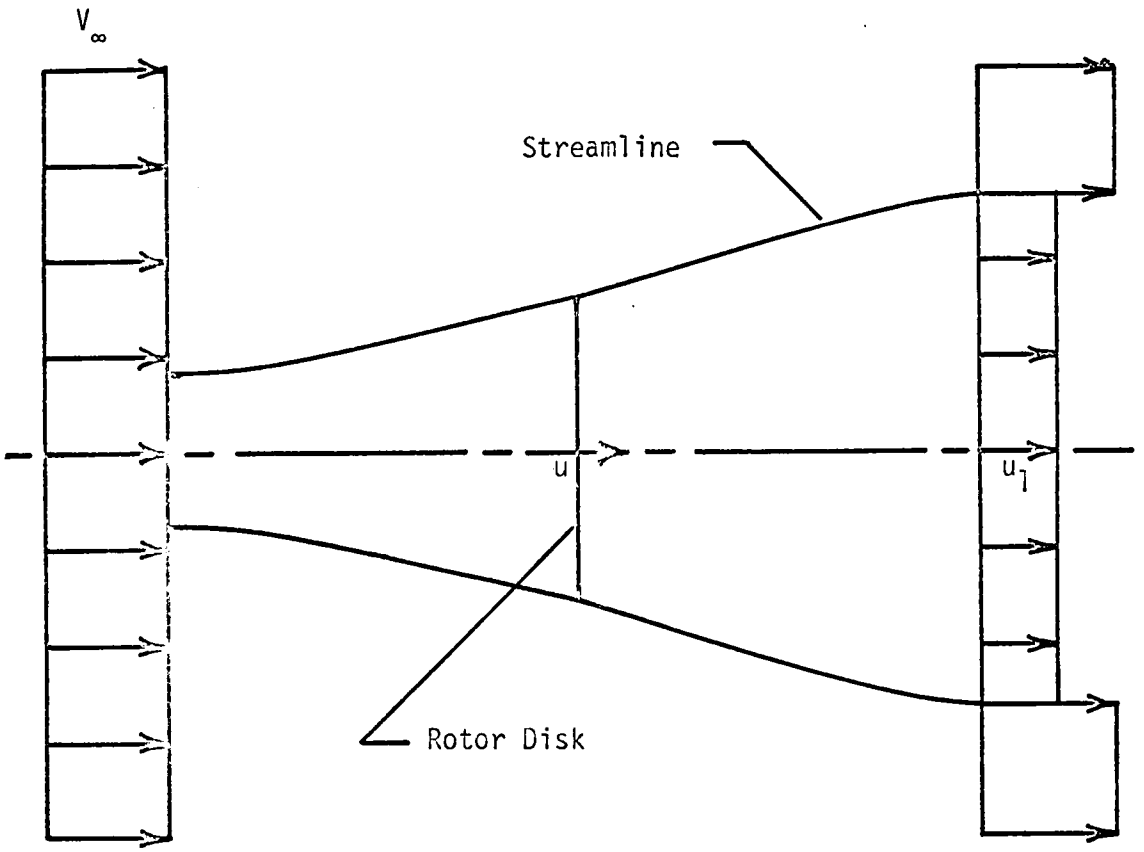

Figure 2. One Dimensional Flow Past a Wind Turbine. (from Reference 8)

C_p has a maximum value of 0.593 when a = 1/3.

A real windmill imparts a rotational velocity to the wake in addition to the axial momentum change. The losses due to induced angular momentum are greatest at low tip speed ratios (X).

$$X \equiv \frac{\Omega R}{V_\infty}$$

Referring again to Fig. 1, it is seen that high speed wind turbines exhibit higher values of C_p. However, at values of X above 6 the effects of aerodynamic friction cause the efficiency to drop. Thus, it is imperative to have blades with good L/D characteristics in high speed wind turbines.

Wilson and Lissaman [8] present a computer program designed to allow rapid comparison of the aerodynamic performance of horizontal wind turbines. Their program includes models for tip losses and hub losses, and uses a modified blade element theory approach.

Much research has been done on the use of ducts to increase wind turbine performance. According to Oman and Foreman [9], dynamic stability problems of large rotors limit the conventional wind turbine to a size of about 1 MW. By use of a diffuser duct, rotor disc axial velocity can be increased to provide up to four times the power output for the same size rotor.

Smulders [10] reports that small airfoils added to the rotor tips can produce up to twice the conventional power output, using only 2 per cent of the material needed for a diffuser duct. Figure 3 illustrates a duct and the tips.

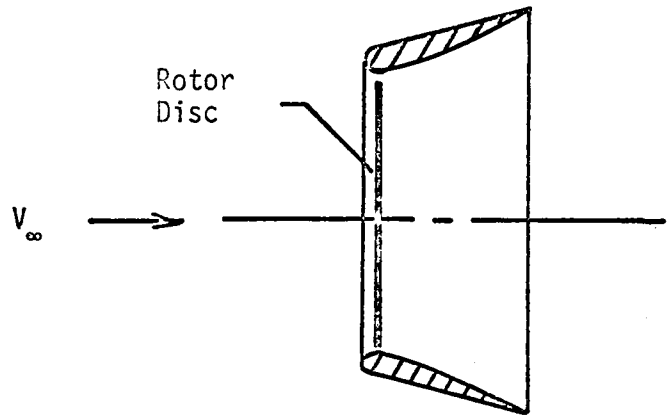

Ducted Wind Turbine

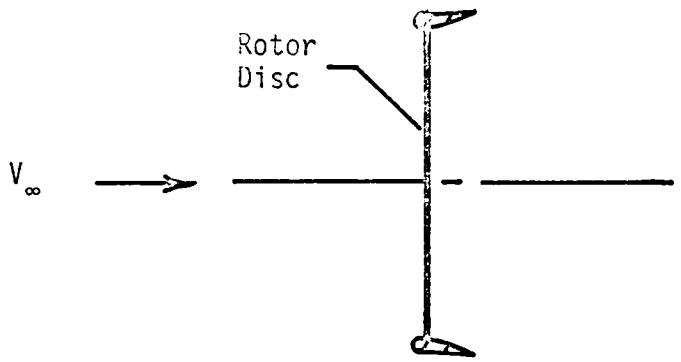

Rotor with Tips

Figure 3. Rotor Augmentation Devices.

Wind Energy Conversion and Storage

Since a conventional horizontal axis wind turbine can extract 59 per cent of the wind's kinetic energy at best, and since the wind is not always blowing, research is also being directed at the problem of energy conversion and storage.

Two of the most common forms of energy conversion are the direct drive of pumps and the generation of electricity. Energy storage for these systems consists of holding tanks and batteries, respectively.

Zlotnic [11] reports on recent advances in energy storage in electro-chemical, flywheel, and compressed air systems.

Blanton [12] describes a composite storage system using both batteries and thermal (ice) storage. This system (Fig. 4) uses a small battery storage system to run air circulating fans, while an ice storage system stores the bulk of the energy needed to cool an apple storage facility. His design will be used in conjunction with the Electro WVG-120G wind turbine described in this thesis.

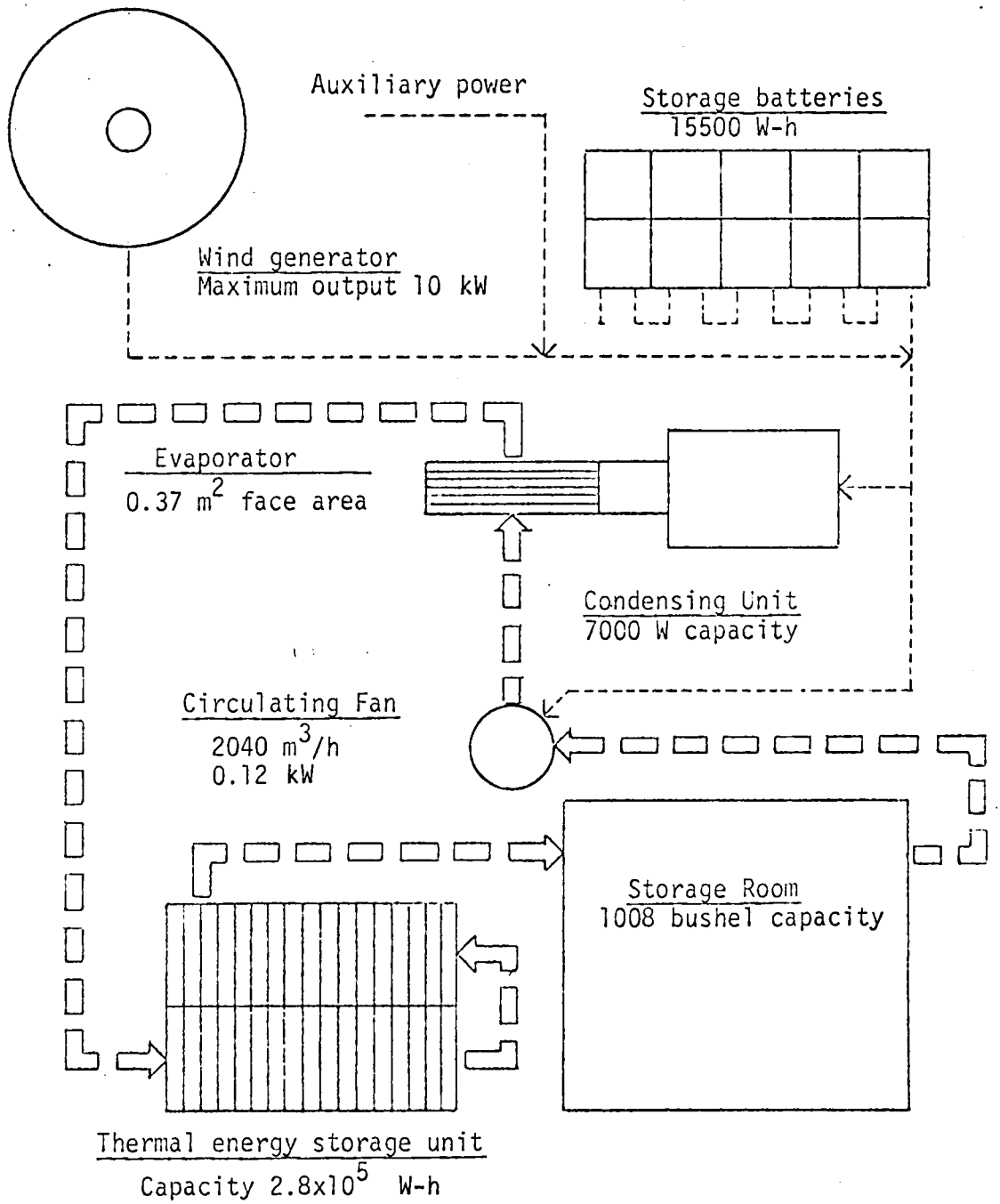

Figure 4. Cooling system schematic.
(From Reference 12)

IX. DESCRIPTION OF SYSTEM

Overview

The Electro WVG-120G wind generator and a transportable test center were temporarily erected on the VPI&SU campus to provide a convenient location for initial evaluation of the windmill. Figure 5 illustrates the site and the complete windmill test system.

The wind turbine was supported by a 27 m (90 ft) guyed tower. Two anemometers were mounted on either side of the tower at a height of 21 m (70 ft). This location placed the anemometers 3 m (10 ft) below the swept area of the blades. A weatherproof control box mounted at the base of the tower contains a drive motor which positions the tail fin of the wind turbine via a steel cable routed up the interior of the tower.

Figure 6 shows (from left to right) the instrument building, the resistive load bank shelter, and the battery shelter. Figure 7 is a block diagram of the electrical distribution system as described in this thesis. The instrument building contains the rectifiers and the main control box of the wind turbine, as well as all instrumentation. The building is heated and cooled, as necessary, to maintain a proper environment for electronic equipment. Each subsystem is described in detail in the following sections.

The windmill, tower, and buildings were moved in late Summer 1977 to the apple storage site located at the VPI&SU Horticulture Farm.

Electro WVG-120G Wind Generator

The Electro WVG-120G is a three-bladed, horizontal-axis wind turbine with a maximum rated output of 10 kW. Although it is called

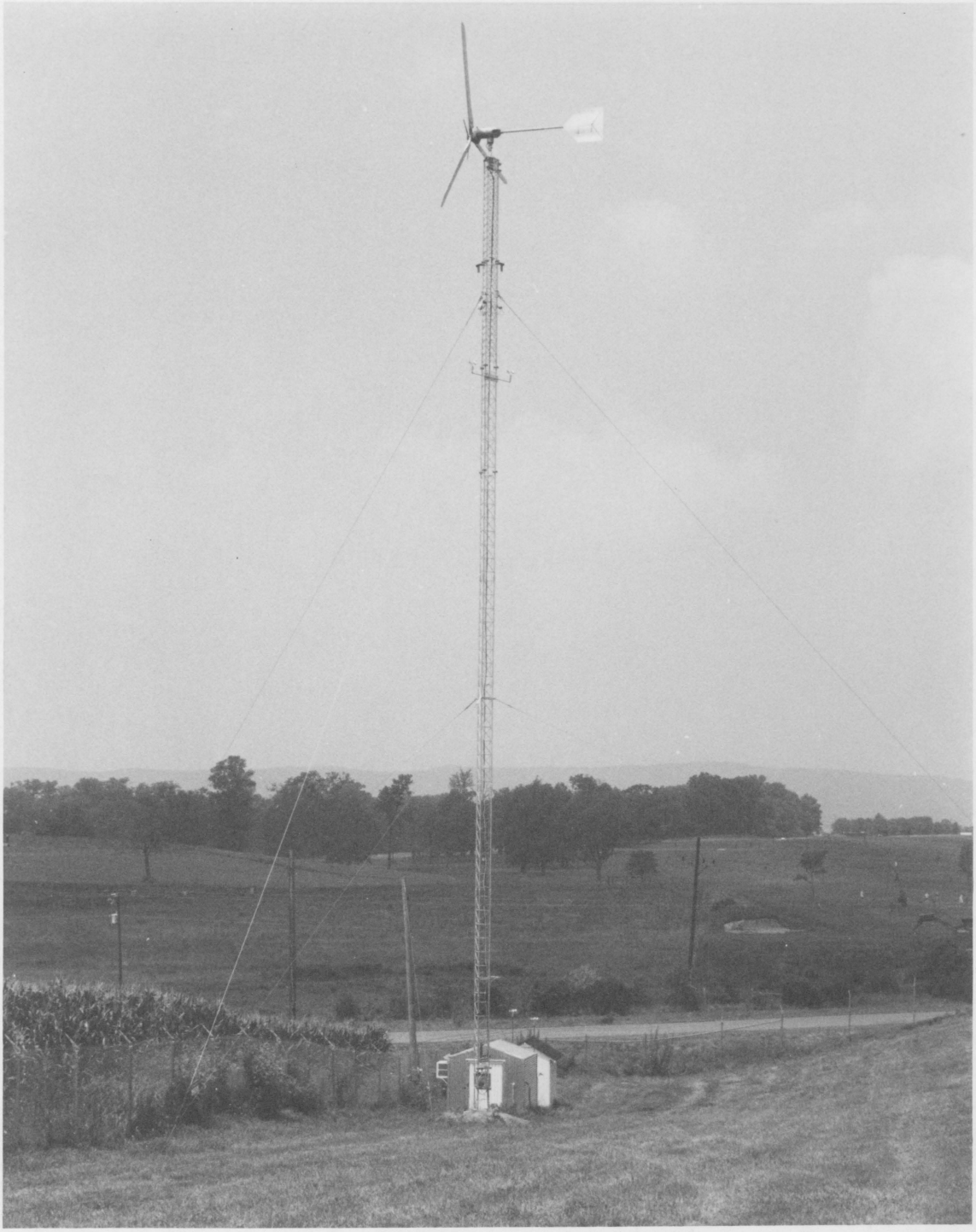

Figure 5. WVG-120G Wind Turbine and Test Site.

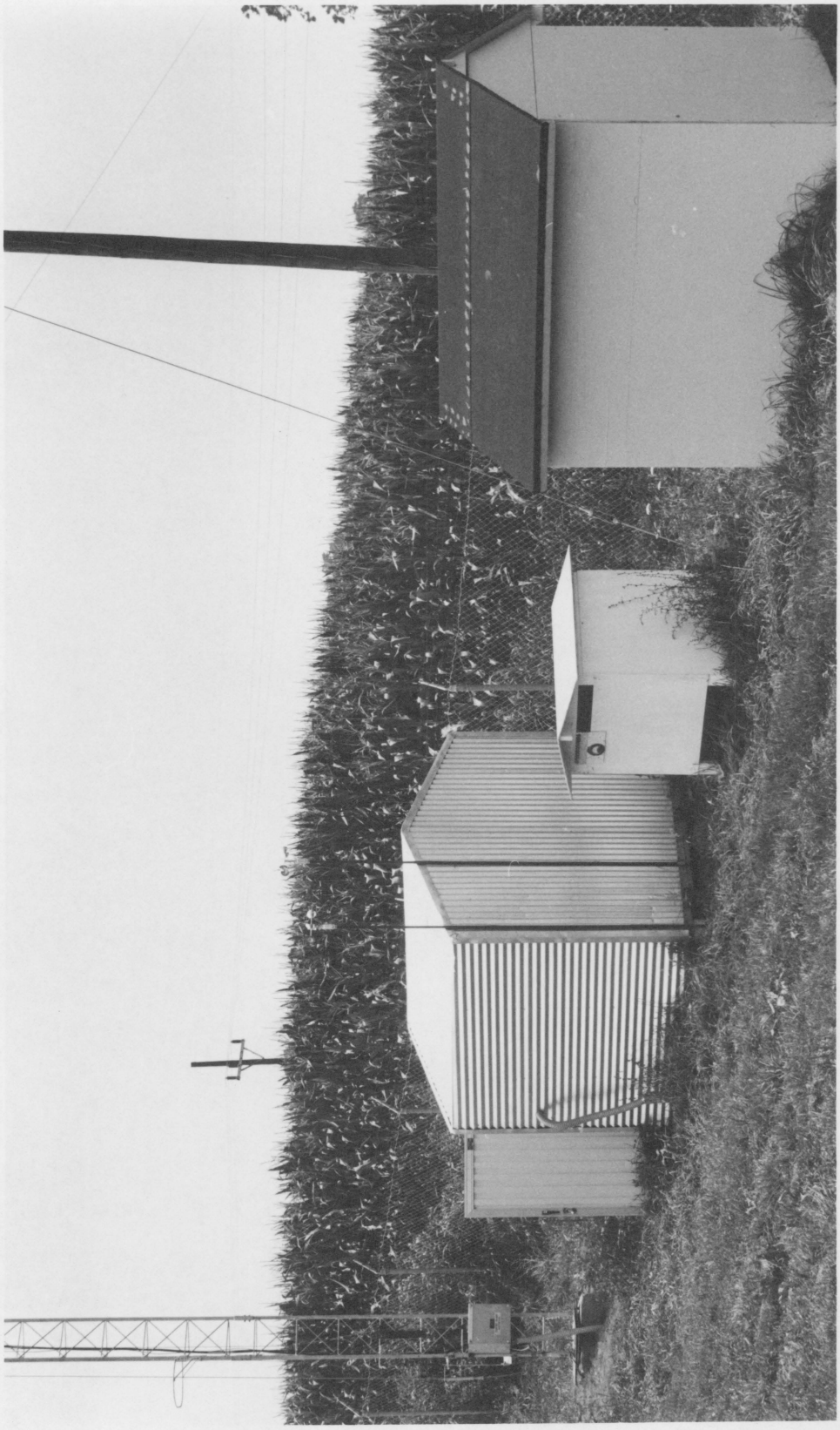

Figure 6. Test Site Building Layout.

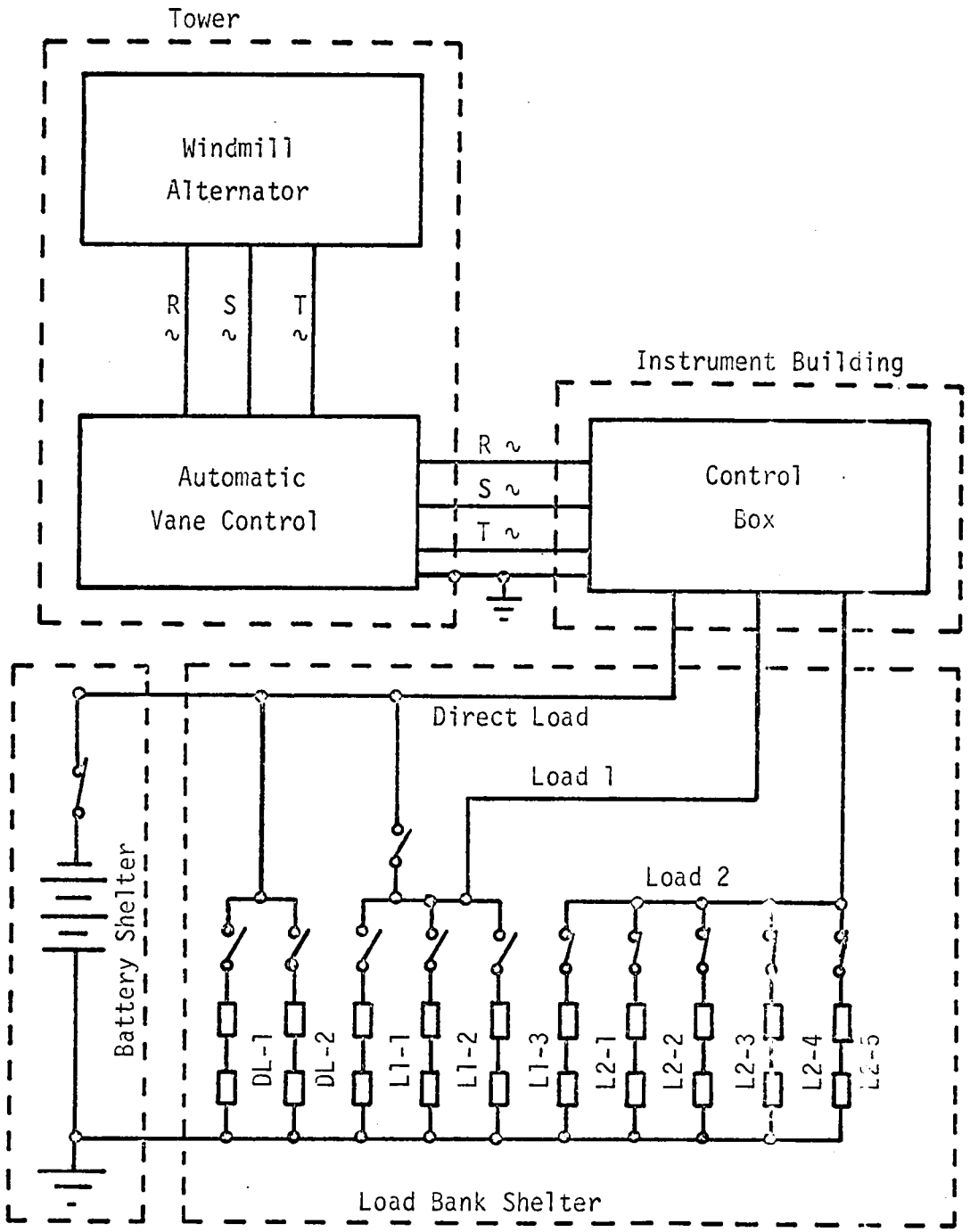

Figure 7. Electrical Power Distribution.

a wind generator by the manufacturer, the primary electrical output is 3-phase alternating current. Specifications for the wind generator are listed in Appendix A.

The blades are made of laminated fir and are roughly shaped to a Clark-Y airfoil (Fig. 8). Note that the leading edge is essentially blunt. Blade measurements taken from one of the blades delivered with the windmill are listed in Table 1. Corresponding specifications for a Clark-Y airfoil are listed at the bottom of the table.

The pitch (θ) of the blades at the root is 14.5° and varies nearly linearly to 5° at the tip. Referring to Fig. 9, it is seen that the angle of attack (α) of a blade element is dependent on the rotational speed, the radius of the element, the pitch of the blade, and the wind speed at the rotor plane.

Maximum performance of the Clark-Y airfoil is obtained at an angle of attack of about 0.5° [13]. The Clark-Y airfoil maintains a fairly good L/D ratio (> 16) from an angle of attack of -3° to 8°.

Figure 10 shows the angle of attack of the WVG-120G blades as a function of section radius for several values of tip speed ratio. Since 75 per cent of the wind energy is contained in the area swept by the outer half of the blades, it is paramount that this portion of the blades, at least, operates efficiently. Figure 10 shows that the angle of attack of the outer 50 per cent of the WVG-120G blades is in the desirable range at tip speed ratios from 6 to 8.

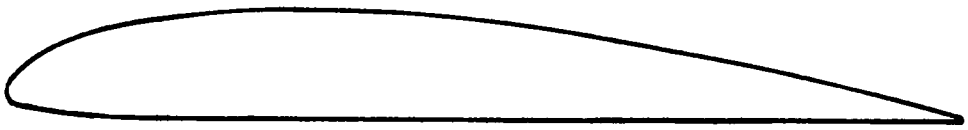

Clark-Y Airfoil

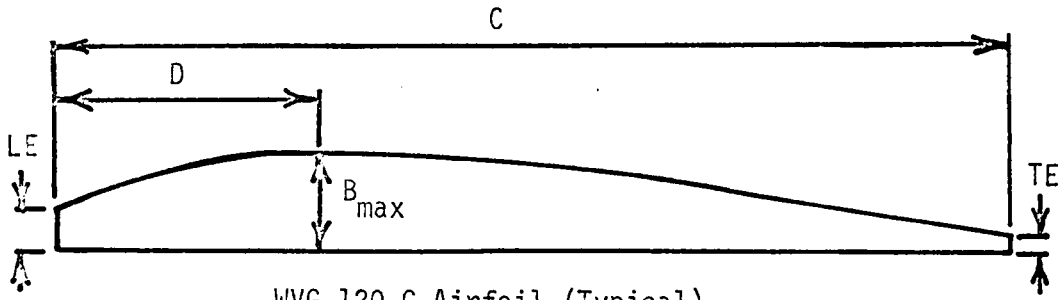

WVG-120 G Airfoil (Typical)

Figure 8. Clark-Y and WVG-120 G Airfoils.

Table 1

WVG-120G Blade Measurements and Clark-Y Specifications

WVG-120G Blade Measurements (Note):

Distance From Root, m(in)	C, mm(in)	LE/C	TE/C	B_{max}/C	D/C
0.00(0)	198(7.8)	0.24	0.17	.24	0.0
0.31(12)	200(7.9)	0.19	.13	.19	.13
0.61(24)	200(7.9)	0.13	.05	.17	.31
0.91(36)	200(7.9)	0.06	.01	.12	.31
1.22(48)	200(7.9)	0.06	.01	.11	.31
1.52(60)	200(7.9)	0.06	.01	.09	.33
1.83(72)	200(7.9)	0.06	.01	.09	.35
2.13(84)	200(7.9)	0.04	.01	.10	.35
2.44(96)	195(7.7)	0.04	.01	.08	.35
2.59(102)	195(7.7)	0.04	.01	.11	.38
2.74(108)	178(7.0)	0.04	.01	.11	.38
2.82(111)	150(5.9)	0.05	.03	.11	.39
2.90(114)	117(4.6)	0.07	.04	.11	.43
2.92(115)	61(2.4)	0.12	.12	.11	.58

Clark-Y Specifications:

LE/C = 0.02 (radius)

TE/C = 0.001

B_{max}/C = 0.12

D/C = 0.30

Note: Refer to Figure 8 for symbol identification.

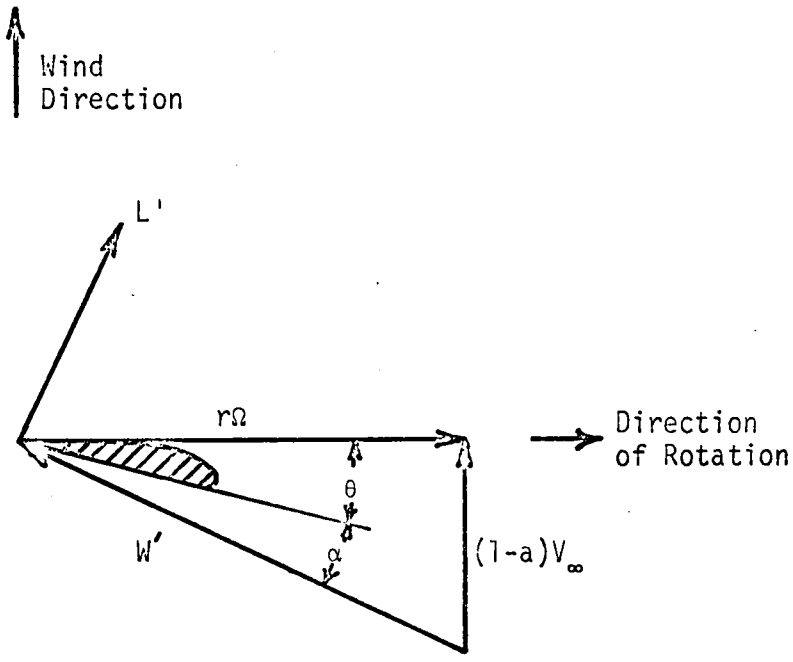

Figure 9. Blade Element Velocity Triangle.
(from Reference 8)

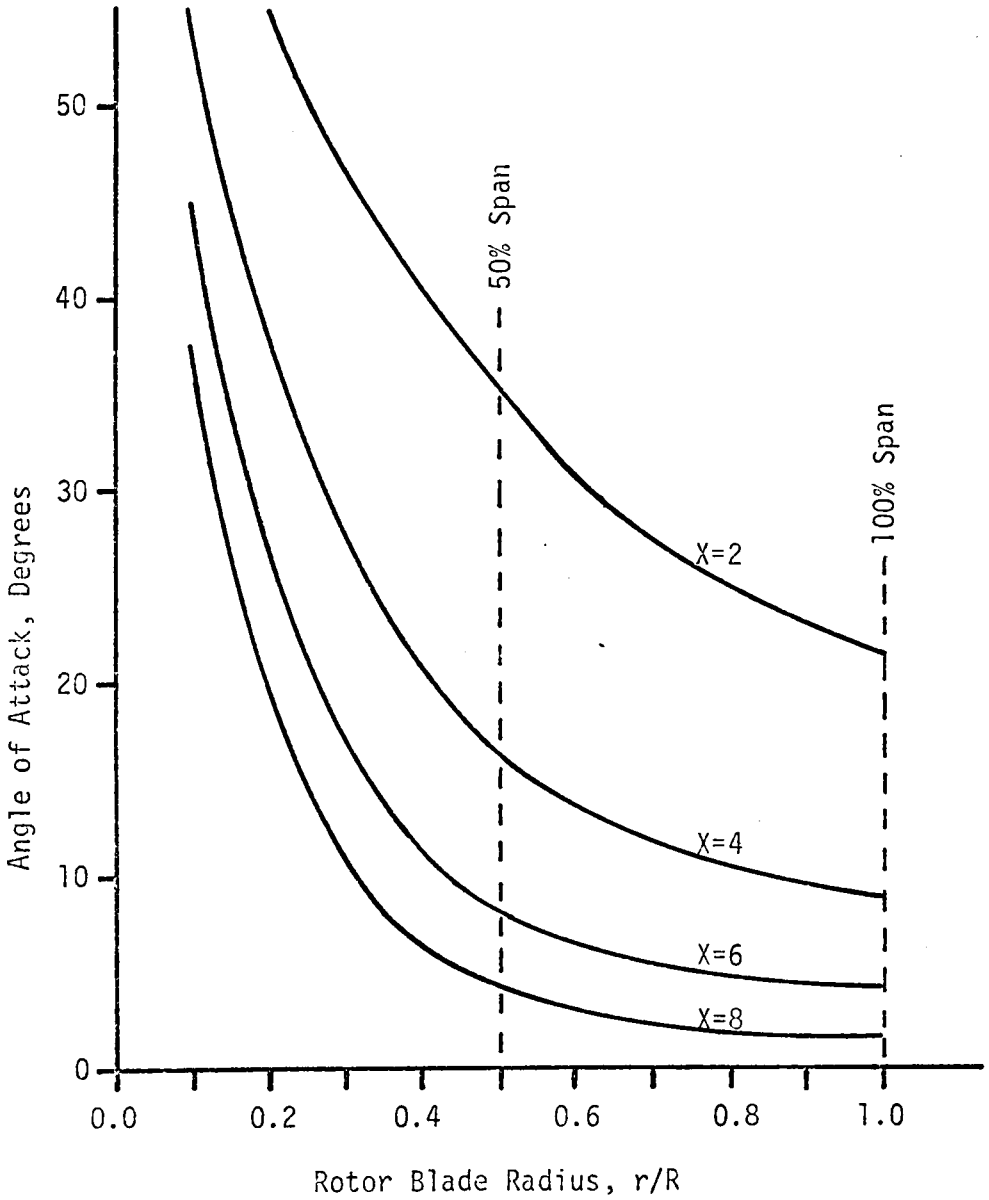

Note: Values shown assume no axial interference and no pitch change by feathering mechanism.

Figure 10. Angle of Attack vs. Radius at Various Values of X.

Performance Predictions

The wind turbine analysis program described in Reference [8] was modified by Mr. Reg Figard of the VPI&SU Aerospace and Ocean Engineering Department for use on the VPI&SU computer. Results from this program using the WVG-120G blade geometry and the Clark-Y airfoil are plotted on Fig. 11 for tip speed ratios of 4 and 8, along with the output power curve of an ideal windmill with the same blade radius. Note that these curves only represent power extracted from the wind and do not include mechanical or electrical losses incurred during energy conversion and transmission.

Control System

Since a windmill must operate over a wide range of wind speeds, some provision must be made to match the load to the available power in the wind, and to vary the operating characteristics of the wind turbine. The control system provides this capability, as well as providing automatic shutdown in out-of-specification conditions. The electrical system and automatic control schematic is shown in Appendix B.

When charging a battery the load matching is simplified since the battery can accept a large range of charging current at a relatively constant voltage. However, protection must still be provided against overcharging or overspeed of the wind turbine. If the windmill is directly powering a resistive load, the control problem is much more difficult. As the wind speed changes, the windmill speed

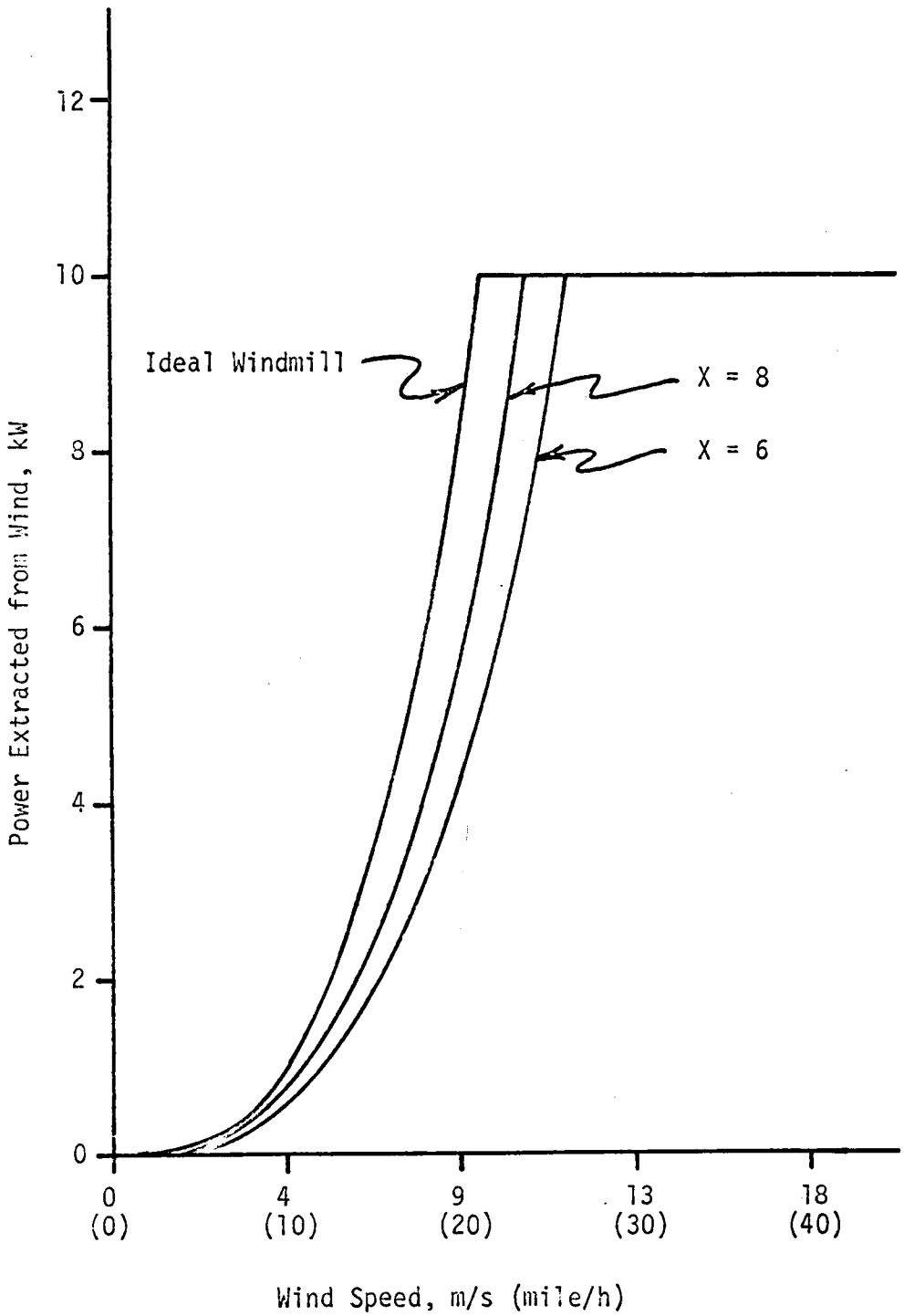

Figure 11. Computer Prediction of WVG-120G Performance.

and voltage vary, as well as the current. A load that can dissipate the rated output draws too much current at low wind speeds, preventing the wind turbine from reaching optimum rotational speed.

The Electro machine was furnished with the capability to charge batteries or to directly power a load. The resistive load was divided into three sections; a "Direct Load" to be connected at all times, "Load 1" to be connected at higher wind speeds, and "Load 2" to be connected at even greater wind speeds. The load bank is described in detail in the next section.

To achieve the switching necessary to insure that the proper load is connected, relays were provided that sense the output voltage. When the voltage reaches 120- 135 V DC, Load 1 is connected. When the voltage rises to 140- 155 V, Load 2 is added to the circuit. Figure B-2 illustrates the switching relays and load contactors. During initial testing with the resistive loads, severe relay chatter was observed which necessitated the addition of a 450 μF capacitor across each coil. This modification, shown in Fig. B-2, made the load switching much smoother. With the battery bank in place it was necessary to protect it from being overcharged. This was done by removing the Direct Load and Load 1 from the system, allowing Load 2 to be connected automatically at 140- 155 V.

The Electro WVG-120G is equipped with a propeller feathering mechanism that is centrifugally actuated at high rotational speeds. The feathering mechanism helps to prevent overspeed in high winds or in the event that the load is lost. Data are not available on the

pitch change vs RPM, but pitch can increase about 10° from the initial setting.

There are three conditions which will cause the automatic control to actuate the cable drive system mounted at the base of the tower, turning the windmill fully or partially out of the wind. These are overvoltage, overcurrent, and high wind. The overvoltage circuit energizes at about 160 V, the overcurrent at 65 A, and the wind sensor at about 18 m/s (40 mi/hr). All of the above limits can be adjusted about 10%, although caution is recommended by the manufacturer if they are increased. Once the windmill is turned out of the wind, it will remain thus until the automatic timer energizes the starting circuit. This occurs every 6 hours.

Resistive Load Bank

The resistive load bank, shown in Fig. 7, consists of ten pairs of 13.5 ohm heating elements. Each pair is rated at 1 kW at 165 V. The load bank was initially set up according to the windmill manufacturer's recommendations:

Direct Load (DL) - 20%

Load 1 (1) - 30%

Load 2 (2) - 50%

Each pair of resistors is connected by a knife switch to the circuit, allowing the operator to vary the load. This feature is useful for studying the effects of load size and load switching on system

performance. The resistors are mounted in ceramic light sockets allowing easy substitution of various-sized units for further experimentation with load sizing.

Appendix C contains power dissipation data for three different sizes of resistive loads. Figures 20 through 25 show the effect of different resistive loads on the performance of the wind generator.

Battery Bank

The battery bank used was a modified Nife C3600 nickel cadmium battery consisting of 91 cells. The specifications for this battery are contained in Appendix D.

Nickel cadmium batteries are ideally suited for windmill applications because they are not damaged by deep discharging, their usable voltage range is relatively large, and they can be charged indefinitely if the maximum voltage is not exceeded. The chief drawback to nickel cadmium batteries is that they cost much more than lead acid batteries.

Referring to Appendix D, the battery system has the following characteristics -

Maximum Peak Voltage: 157 V

Maximum Continuous Voltage: 141 V

Minimum Allowable Voltage: 100 V

Maximum Charging Current: 34.6 A

Efficiency: $= \frac{P_{discharge}}{P_{charge}} = \frac{1.2x30x4}{1.55x34.6x5} = 54\%$

Average Discharge Voltage: 1.2 x 91 = 110 V

Available Stored Energy: 13.1 kW-h

The efficiency and available stored energy can be increased by 5 per cent if the discharge rate is reduced to 15 amps or less.

Electrical Output Measurement System

Since the final criterion in judging whether a wind generator is operating correctly is its power output, a system was developed to display and record critical electrical parameters. Figure 12 is the block diagram of this system. The parameters measured were voltage, current, frequency (proportional to rotor speed), and power. Strip chart recorders were equipped with event markers which were triggered by contacting anemometers to provide current wind data simultaneously with the electrical output.

It was decided that all parameters to be measured would be converted to a voltage signal to permit easy transmission and scaling, and to facilitate interfacing with standard recording instruments. A data logger may be used in future research which makes signal conditioning even more important. Figure 13 is the schematic of the electrical output signal conditioning circuits. Generator voltage was divided by 1000 through a resistance network. A direct readout was provided by a $\pm$199 mV digital panel meter (DPM) and the millivolt signal was also recorded on a strip chart recorder. Generator current was passed through a 0.001 OHM shunt to provide a voltage signal of 1 mV per Amp. Again, this signal was displayed on a $\pm$199 mV DPM and recorded on a strip chart recorder. The frequency of the windmill alternator was measured using a Beckman frequency counter. A parallel

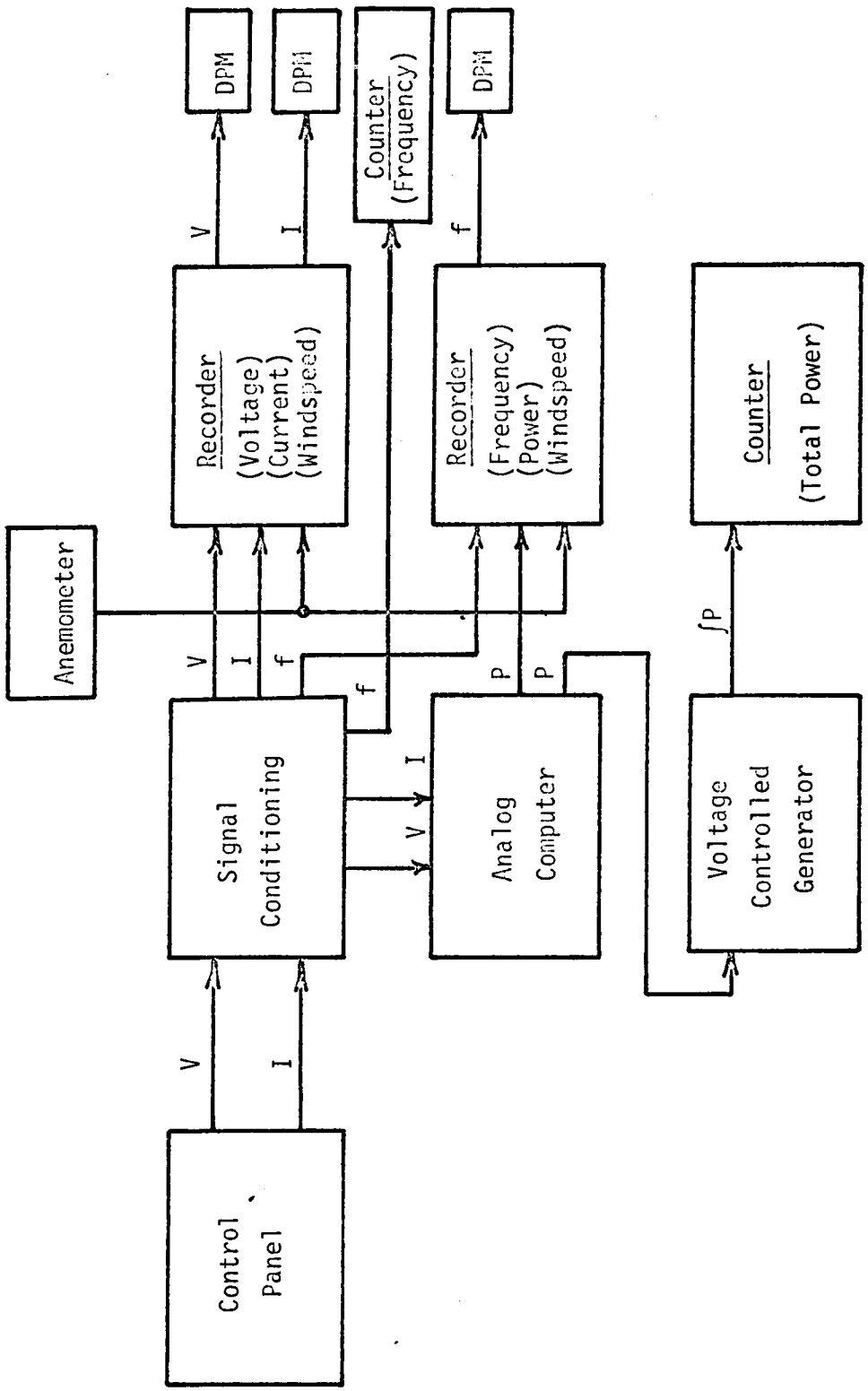

Figure 12. Block Diagram of Performance Measuring System.

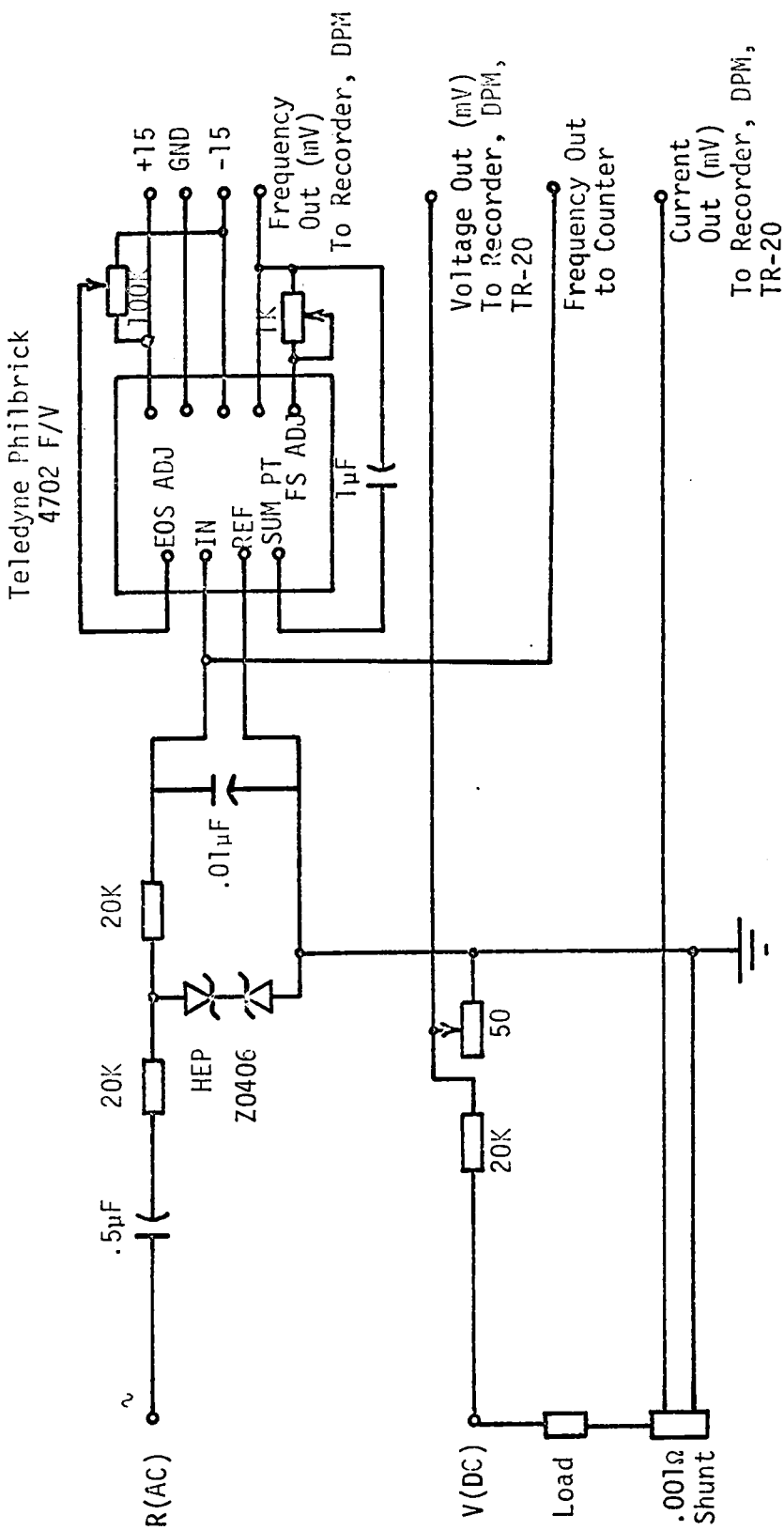

Figure 13. Signal Conditioning Circuit.

system using a Teledyne Philbrick frequency-to-voltage converter (F/V) was employed for a short period of time but failed after the test cases using the resistive load. The output of the F/V was a millivolt level signal that was proportional to the frequency of the generator. The rotor RPM can be obtained by multiplying the frequency by 1.82 (Fig. A1). This number is obtained in the following manner:

$$RPM = (f)(\text{gear ratio})(2/\text{alternator poles})(60\ \text{s/min}) \quad (11)$$

$$RPM = (f)(1/4.12)(2/16)(60)$$

$$RPM = 1.82\ f$$

Measuring power required several steps. The mV level voltage and current signals were amplified and multiplied (Fig. 14) by an EAI TR-20 Analog Computer to provide a signal of 1 mV per watt. This signal was recorded on a strip chart recorder to provide a continuous power record and was input to a Wavetek Model 111 Voltage Controlled Generator (VCG). The frequency of the output signal of the VCG was thus proportional to the power produced. This signal was counted on a Beckman Digital Counter, providing a total count which, when divided by time, was proportional to kW-h produced. During system calibration, this method of measuring power was found to be inaccurate (App. E) and was not used in the test cases. Alternatively, voltage and current values from the recorder were multiplied together to produce power data.

Wind Measurement System

Two types of commercially-available anemometers were used to monitor wind velocity at the test site. The Stewart anemometer is a

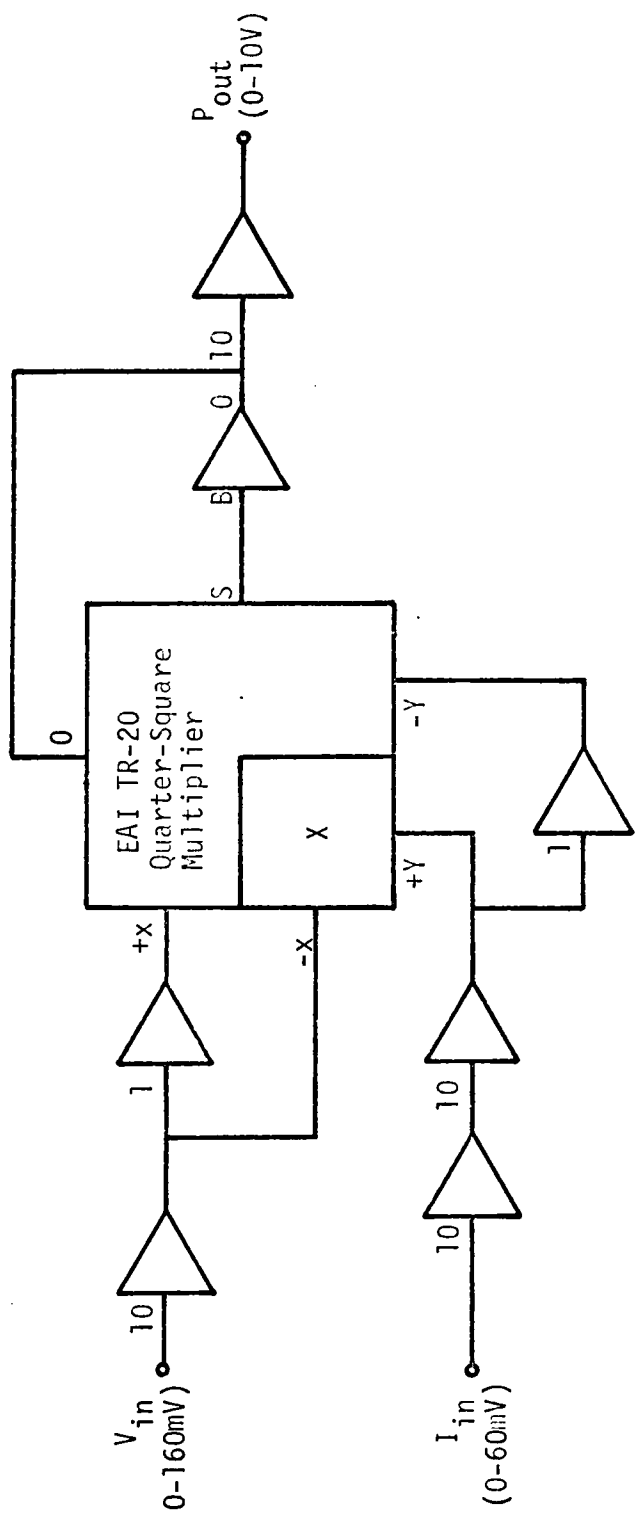

Figure 14. Multiplier Patching Circuit, (V x I = P).

small, lightweight, inexpensive cup anemometer that utilizes a magnetic reed switch to measure the passage of 27 m (1/60 mile) of wind. The Belfort anemometer is a slightly larger, heavier, and more expensive cup anemometer that utilizes mechanical contacts to measure 27 m (1/60 mile) of wind. Although the Belfort model is more sophisticated and has higher quality components, the contacts tend to pit and must be cleaned and adjusted every 60 - 90 days. The Stewart anemometers are virtually maintenance free and have not failed to operate satisfactorily.

Although wind units of 27 m (1/60 mile) are satisfactory for obtaining mean wind information and comparing various sites, that distance represents a relatively long time (approximately 3 s duration at a velocity of 9 m/s (20 mile/h)) and does not provide meaningful short term wind velocity data.

One Stewart anemometer was modified to provide better resolution. The worm and gear were removed and the actuating magnet was mounted on the rotor shaft. Figures 15 and 16 show a Stewart anemometer and the modification. This arrangement provides 16 times better resolution (1.68 m (5.5 ft)).

The recorders sold with the anemometers are of two types. The Stewart odometer is a transitorized, electro-mechanical counter that accumulates total elapsed distance. By dividing by the time between observations one obtains an average wind speed. The Belfort instruments are Rustrak recorders that have been modified to register the contact closings of the anemometer. This recorder permits determination of wind

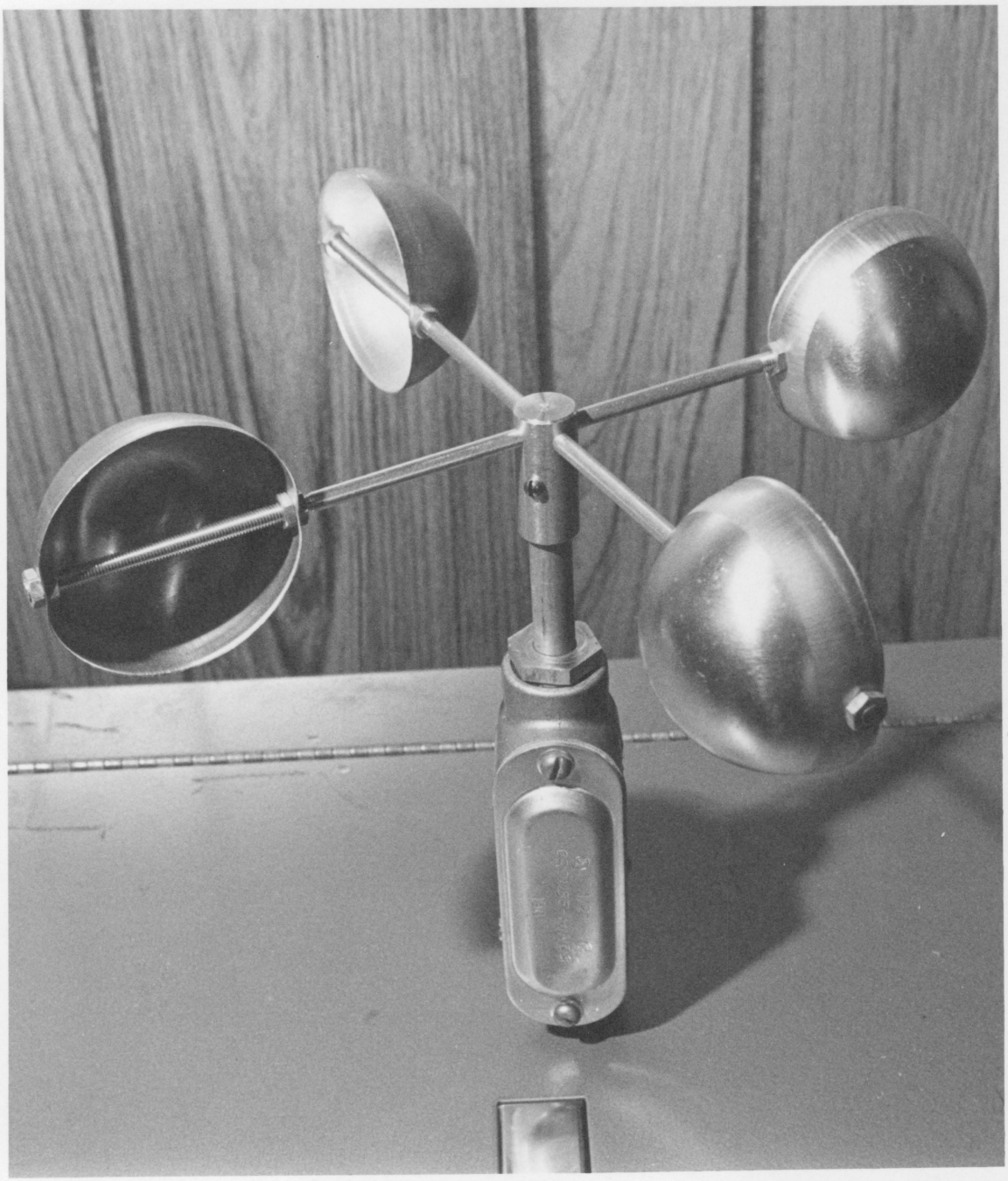

Figure 15. Stewart Anemometer.

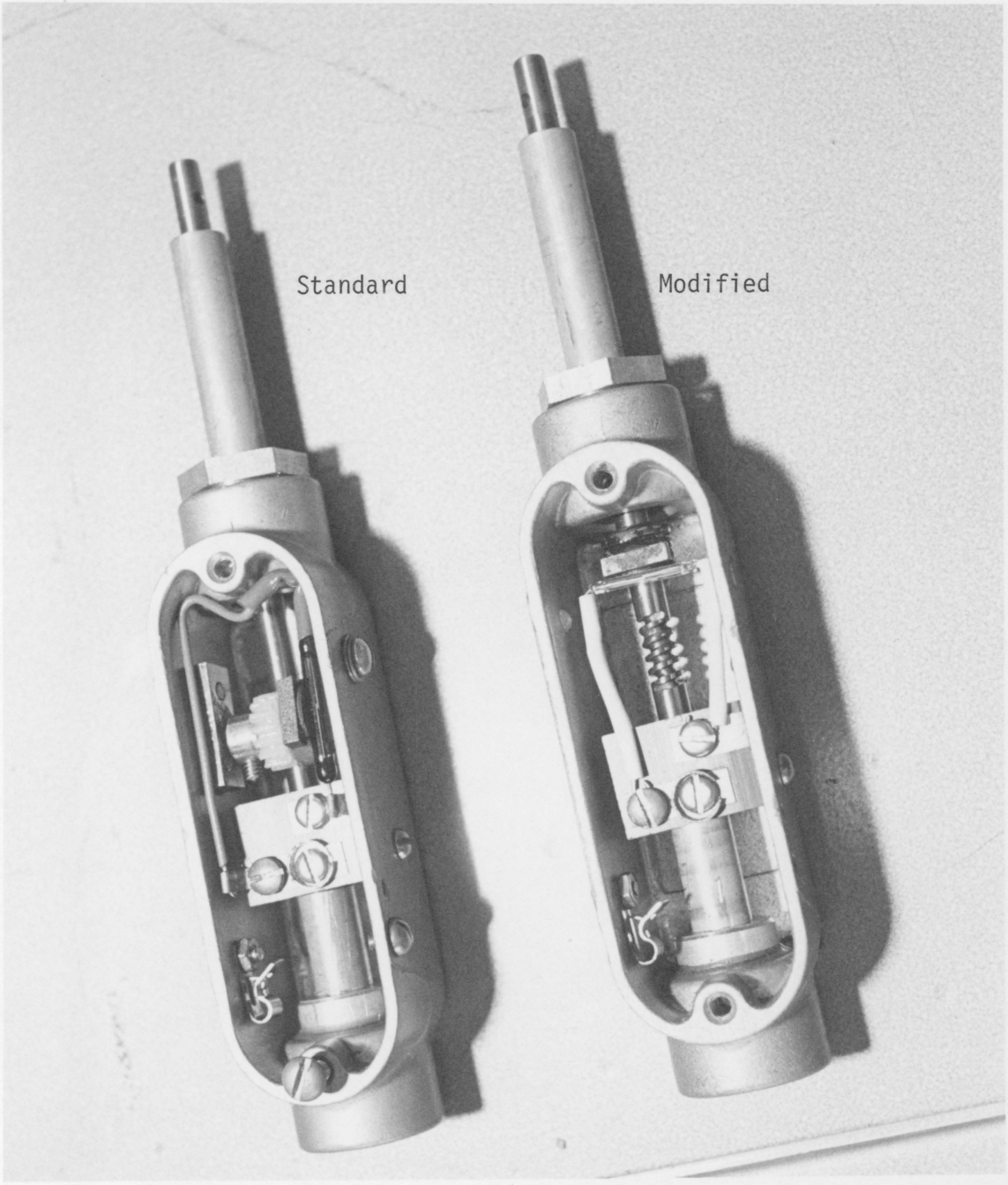

Figure 16. Detail of Stewart Anemometer Modification.

velocity over periods as small as 15 minutes duration. A transistorized switching circuit was designed and added to the Belfort recorders to allow their use with the Stewart anemometers. This circuit, Fig. 17, protects the delicate reed switches from a large current flow from the recorder.

Both types of recorders were used for site selection, in a remote, outdoor environment. During cold, wet weather the Stewart odometer tended to stick and the battery drain on both the odometers and the recorders was excessive. These problems led to development of a solid-state odometer using CMOS and TTL integrated circuit components, Fig. 18. Figure 19 shows the completed counter. A second unit is being developed using 100 per cent CMOS logic components for which the battery drain will be negligible.

Although mean value wind data is useful for initial wind energy site surveys, the total available wind energy can only be determined from a wind speed duration curve, which shows the amount of time the wind speed was above a specified level.

Two sites may have an identical mean wind speed but have vastly different potential for driving wind energy systems. Suppose for example that two sites each have a mean wind speed of 4.5 m/s (10 mile/h). The wind at Site A is 9 m/s (20 mile/h) during half the time and calm during half the time. The wind at Site B is constant at 4.5 m/s (10 mile/h). From equations (2) and (3) the energy in the wind is

$$E = \frac{1}{2} \rho \, AtV_{\infty}^{3} \qquad (12)$$

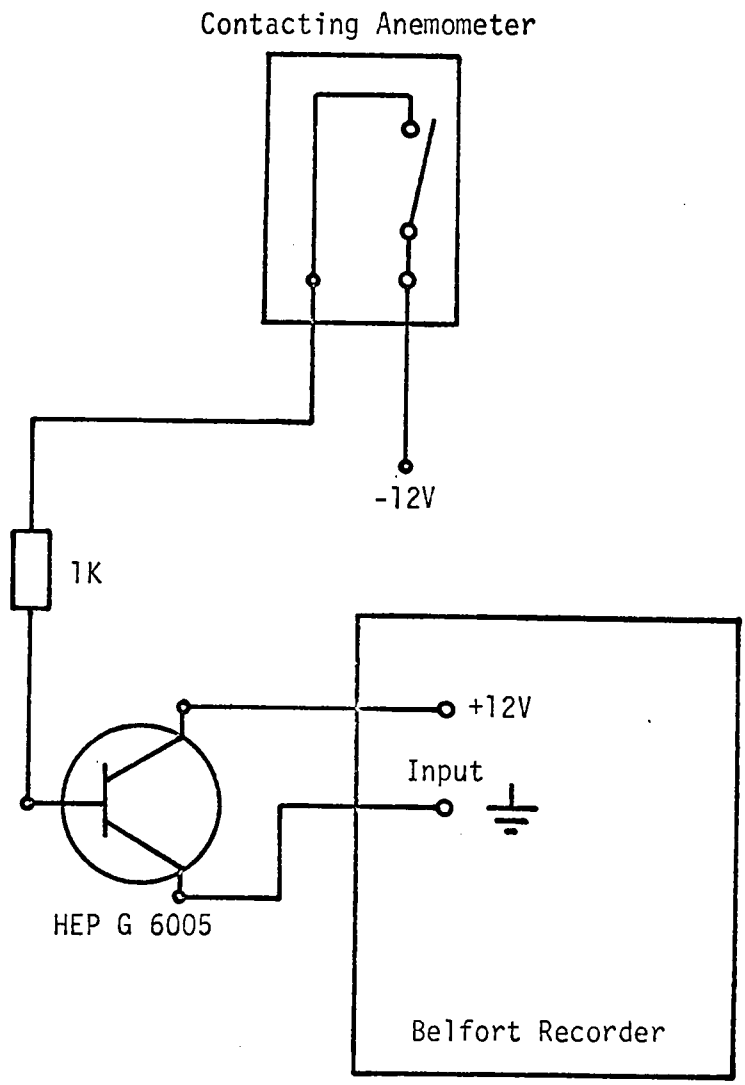

Figure 17. Belfort Recorder Input Modification.

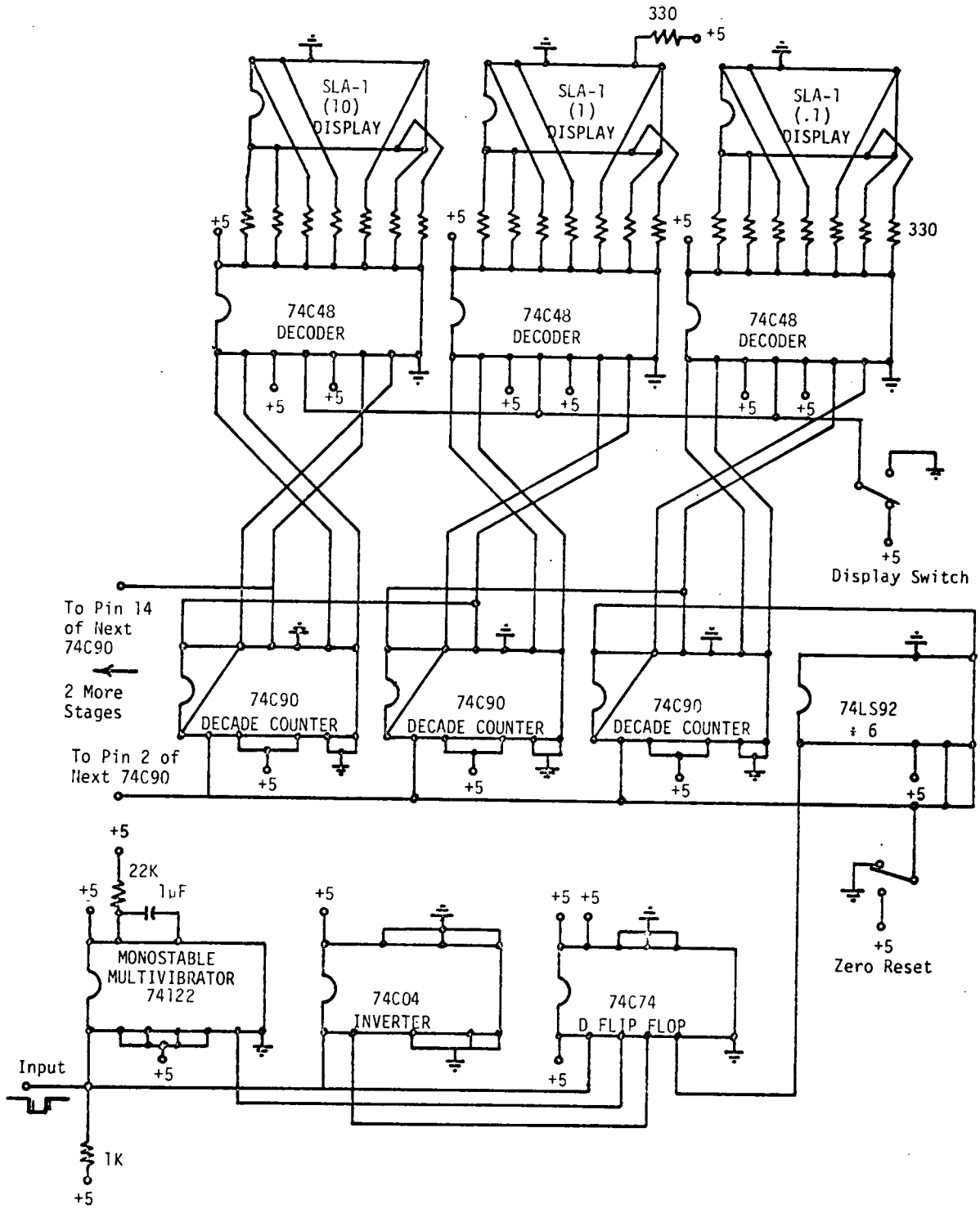

Figure 18. Schematic of Integrated Circuit Odometer.

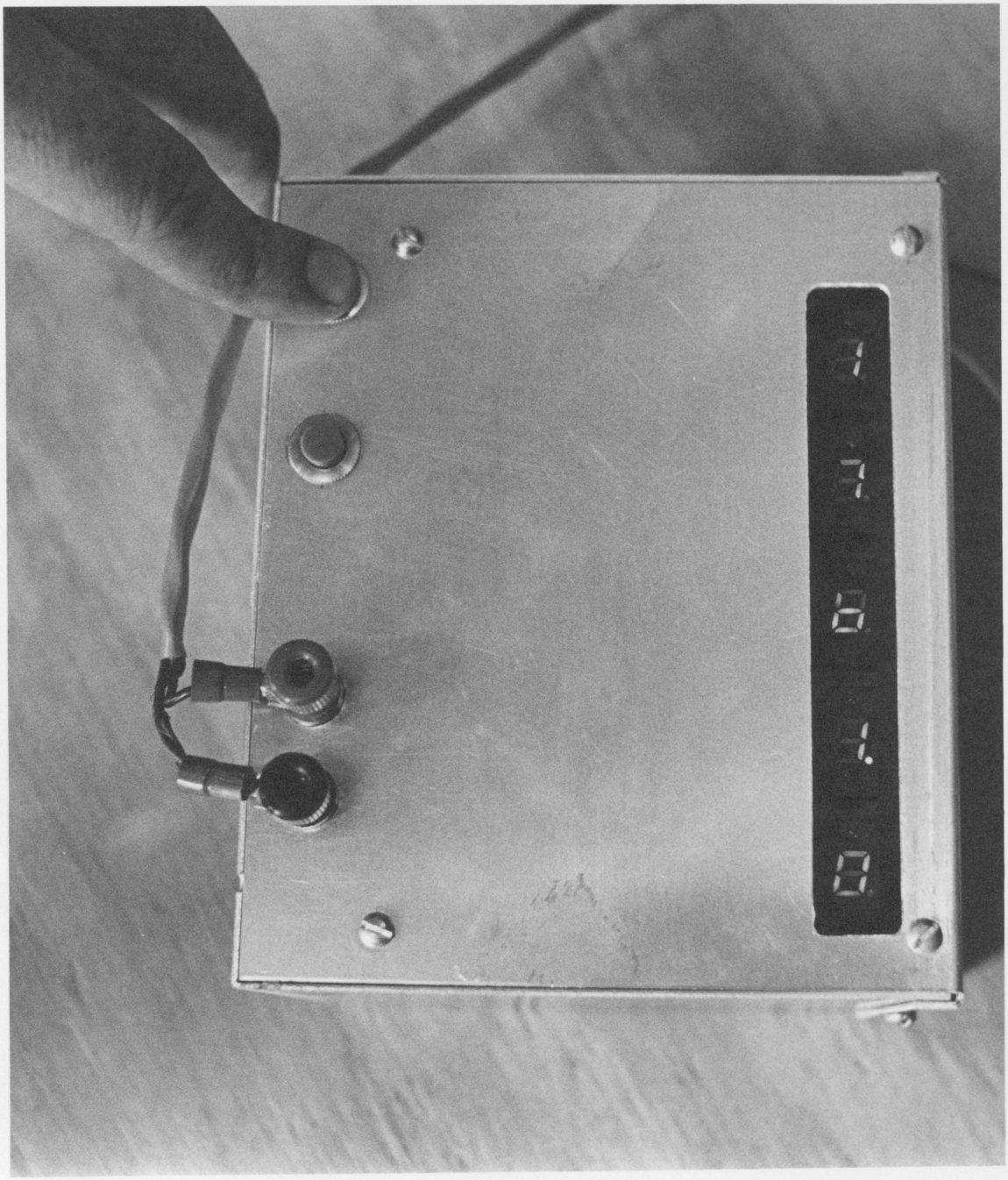

Figure 19. Integrated Circuit Odometer.

Thus

$$E_A = \frac{1}{2}\rho A(t/2)(9)^3 + \frac{1}{2}\rho A(t/2)(0)^3 \qquad (13)$$

and

$$E_B = \frac{1}{2}\rho A(t)(4.5)^3 \qquad (14)$$

Therefore

$$\frac{E_A}{E_B} = \frac{(0.5)(9)^3}{(4.5)^3} = 4 \qquad (15)$$

This effect is most noticeable when comparing sites that have different geographical features or weather patterns. For example, a coastal location may exhibit a strong diurnal variation while an inland site may have fairly uniform wind speed characteristics throughout the day, changing with the passage of weather fronts.

Reed [7] proposes that a sample duration of 15 seconds is an adequate time period for obtaining wind speed samples. This time period can easily be handled by interfacing the solid state counter to a microprocessor. There are devices on the market which will automatically log wind speed-duration data, and at least one battery operated device to accomplish this is being developed.

X. DATA

Performance measurements for 13 separate test cases are recorded in this section. Cases 1 through 7 document the use of the WVG-120G wind turbine to directly power a resistive load, with the load size and switching level being changed between test cases. The last 6 cases are concerned with the use of the windmill to charge the battery bank. The state of charge was the primary variable between cases in these tests.

Table 2 identifies the 13 test cases. Table 3 is a performance data summary which includes the standard deviations of the measured variables. The data for each test case are plotted against wind speed in Figs. 20-32.

Table 2

Performance Test Case Identification

Case	Date	Load Description (Note)
1	8/5/77	Resistive, DL = 0.01 L1 = 0.1 L2 = 0.5 Load Switching Relay Set at 120 V
2	8/6/77	Resistive, DL = 0.11 L1 = 0.1 L2 = 0.5 Load Switching Relay Set at 135 V
3	8/6/77	Resistive, DL = 0.1 L1 = 0.1 L2 = 0.5 Load Switching Relay Set at 135 V
4	8/6/77	Resistive, DL = 0.01 L1 = 0.1 L2 = 0.5 Load Switching Relay Set at 120 V
5	8/6/77	Resistive, DL = 0.11 L1 = 0.1 L2 = 0.5 Load Switching Relay Set at 120 V
6	8/6/77	Resistive, DL + L1 = 0.2 L2 = 0.5 Load Switching Relay Set at 120 V
7	8/17/77	Battery, 92 Cells, 129 - 140 V
8	8/23/77	Battery, 91 Cells, 120 V
9	8/23/77	Battery, 91 Cells, 121 V
10	8/24/77	Battery, 91 Cells, 123 - 126 V
11	8/24/77	Battery, 91 Cells, 130 - 137 V
12	8/24/77	Battery, 91 Cells, 135 - 136 V
13	8/24/77	Battery, 91 Cells, 135 - 138 V

Note: Resistive loads stated in fraction of generator rated output.

Table 3

Performance Data Summary
(Mean Value/Standard Deviation)

Case No.	Wind m/s(mile/h)	Occurrences	Voltage V	Current A	Power W	Tip Speed Ratio
1	2.7(6)	15	86/18	.4/.1	31/13	8.1/2.6
	3.6(8)	65	106/15	.6/.8	60/93	7.2/.8
	4.5(10)	20	114/7	2.2/2.2	255/253	6.4/.6
2	2.7(6)	5	24/5	1.3/.2	32/11	4.0/.4
	3.6(8)	25	31/6	1.6/.3	52/19	3.3/.4
	4.5(10)	40	49/8	2.4/.3	121/37	3.5/.3
	5.4(12)	25	71/15	3.5/.5	255/85	3.7/.1
	6.3(14)	5	70/10	3.4/.5	240/72	3.1/.4
3	3.6(8)	5	38/5	1.7/.1	64/13	3.8/.3
	4.5(10)	20	67/27	2.9/.9	221/157	4.4/1.0
	5.4(12)	25	89/25	4.0/1.7	384/275	4.3/1.1
	6.3(14)	35	111/19	5.2/1.9	599/307	4.4/.6
	7.2(16)	15	125/9	7.0/2.5	887/364	4.1/.3
4	3.6(8)	35	99/19	1.1/1.3	116/147	7.0/.7
	4.5(10)	40	108/8	2.6/2.2	321/269	5.7/1.1
	5.4(12)	20	107/6	3.7/2.2	397/245	5.0/.4
	6.3(14)	5	109/6	4.3/2.0	476/226	4.3/.3
5	2.7(6)	5	17/2	1.0/.0	17/2	3.2/.2
	3.6(8)	30	41/19	1.7/.9	88/89	3.8/1.1
	4.5(10)	45	54/11	2.6/.4	145/56	3.7/.5
	5.4(12)	10	85/22	4.5/2.0	417/303	8.1/.8
	6.3(14)	10	72/8	3.6/.3	265/44	3.1/.2
6	2.7(6)	5	18/4	1.4/.4	25/13	3.8/.6
	3.6(8)	10	19/3	1.7/.3	32/11	2.7/.2
	4.5(10)	40	25/6	2.0/.5	53/23	2.5/.5
	5.4(12)	40	37/4	3.1/.3	115/27	2.5/.4
	6.3(14)	5	44/1	3.9/.1	171/7	2.5/.1
7	2.3(5)	1	129/-	.0/-	.0/-	
	2.7(6)	3	131/1	.0/.1	4/7	
	3.1(7)	8	131/1	1.0/.7	131/87	
	3.6(8)	22	131/1	1.3/.6	168/73	
	4.1(9)	29	131/2	2.9/.9	369/127	
	4.5(10)	37	133/3	4.4/1.3	589/174	
	4.9(11)	31	134/2	5.7/1.3	765/174	

Case No.	Wind m/s(mile/h)	Occurrences	Voltage V	Current A	Power W	Tip Speed Ratio
7	5.4(12)	22	136/2	8.2/1.2	1114/170	
	5.9(13)	17	137/2	9.2/1.3	1267/173	
	6.3(14)	11	137/1	10.2/.9	1399/137	
	6.7(15)	3	138/0	12.5/.2	1725/24	
	7.2(16)	1	139/-	15.3/-	2127/-	
	7.7(17)	1	140/-	15.3/-	2142/-	
8	2.7(6)	1	120/-	.3/-	36/-	9.7/-
	3.1(7)	4	120/0	1.0/.4	125/47	8.7/.4
	3.6(8)	7	120/0	1.5/.4	175/49	7.9/.3
	4.1(9)	11	120/0	2.7/.5	327/61	7.3/.2
	4.5(10)	6	120/0	3.5/.4	416/44	6.7/.1
	4.9(11)	1	120/-	4.8/-	576/-	6.1/-
9	1.8(4)	2	121/0	0/0	0/0	9.5/0
	2.3(5)	6	121/0	.1/.2	10/25	9.2/.9
	2.7(6)	4	121/0	.1/.3	15/31	8.6/.9
	3.1(7)	6	121/0	.7/.9	89/109	8.3/.7
	3.6(8)	7	121/0	1.2/.6	126/56	7.8/.3
	4.1(9)	4	121/0	3.0/.2	363/247	7.5/0
10	3.1(7)	1	123/-	.4/-	49/-	7.8/-
	3.6(8)	2	125/2	1.1/.6	131/80	8.0/.4
	4.1(9)	4	124/1	1.2/.8	146/96	6.9/.5
	4.5(10)	6	123/1	2.6/.8	319/93	6.7/1.3
	4.9(11)	7	123/1	4.2/.6	479/48	6.3/.1
	5.4(12)	8	124/1	4.8/.8	590/95	5.7/.2
	5.9(13)	3	124/2	5.9/.1	728/46	5.5/.1
	6.3(14)	2	125/0	6.9/.2	869/26	5.1/.2
	6.7(15)	5	125/1	7.4/.6	922/80	4.8/.1
	7.2(16)	2	126/0	8.1/.1	1019/8	4.7/.1
11	3.1(7)	2	130/0	.6/.2	71/28	7.9/1.2
	3.6(8)	3	131/1	.3/.3	52/37	7.9/.3
	4.1(9)	1	130/-	.5/-	65/-	7.2/-
	4.5(10)	3	133/3	1.9/.5	251/68	7.1/.1
	4.9(11)	2	133/0	5.8/2.4	771/320	6.7/0
	5.4(12)	1	135/-	5.5/-	743/-	6.3/-
	5.9(13)	5	135/1	6.0/1.1	807/145	5.8/1.2
	6.3(14)	0				
	6.7(15)	2	135/1	7.9/1.3	1062/165	5.3/.7
	7.2(16)	0				
	7.7(17)	0				
	8.1(18)	1	137/-	12.0/-	1644/-	4.5/-

Case No.	Wind m/s(mile/h)	Occurrences	Voltage V	Current A	Power W	Tip Speed Ratio
12	4.5(10)	2	135/0	3.0/0.6	405/96	7.1/.2
	4.9(11)	5	135/0	4.1/1.1	556/150	6.7/.2
	5.4(12)	3	135/1	4.8/.7	642/104	6.3/.1
	5.9(13)	2	135/1	5.4/1.6	733/214	5.9/.1
	6.3(14)	1	136/-	6.1/-	830/-	5.5/-
13	3.6(8)	1	135/-	1.8/-	243/-	9.0/-
	4.1(9)	0				
	4.5(10)	1	136/-	3.1/-	422/-	7.4/-
	4.9(11)	2	136/0	3.7/1.3	503/173	6.8/.1
	5.4(12)	1	135/-	3.9/-	527/-	6.1/-
	5.9(13)	1	136/-	5.3/-	721/-	5.8/-
	6.3(14)	2	137/0	7.1/1	966/10	5.6/0
	6.7(15)	1	137/-	6.8/-	932/-	5.3/-
	7.2(16)	1	138/-	8.7/-	1201/-	5.0/-

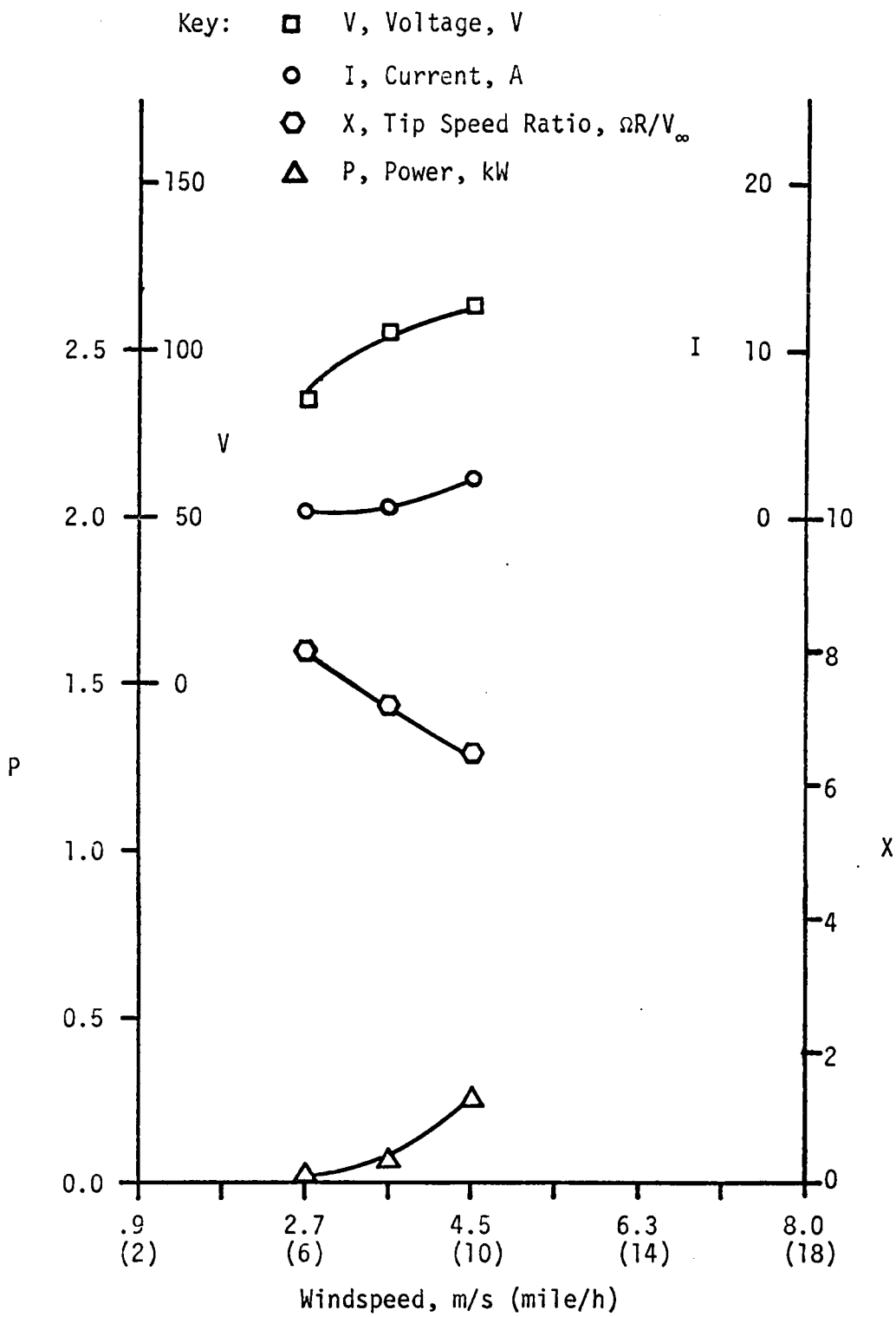

Figure 20. Performance Data, Case 1.

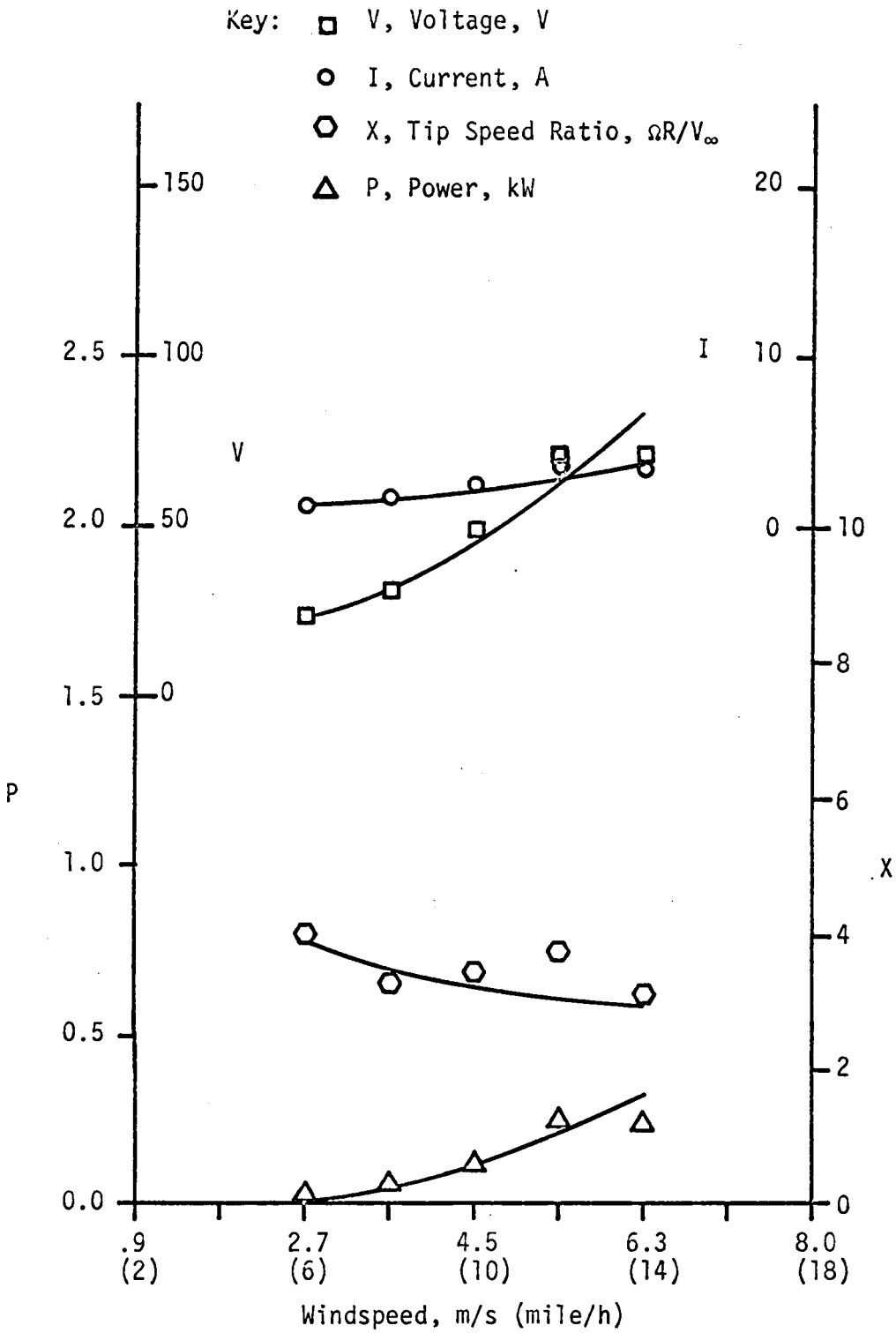

Figure 21. Performance Data, Case 2.

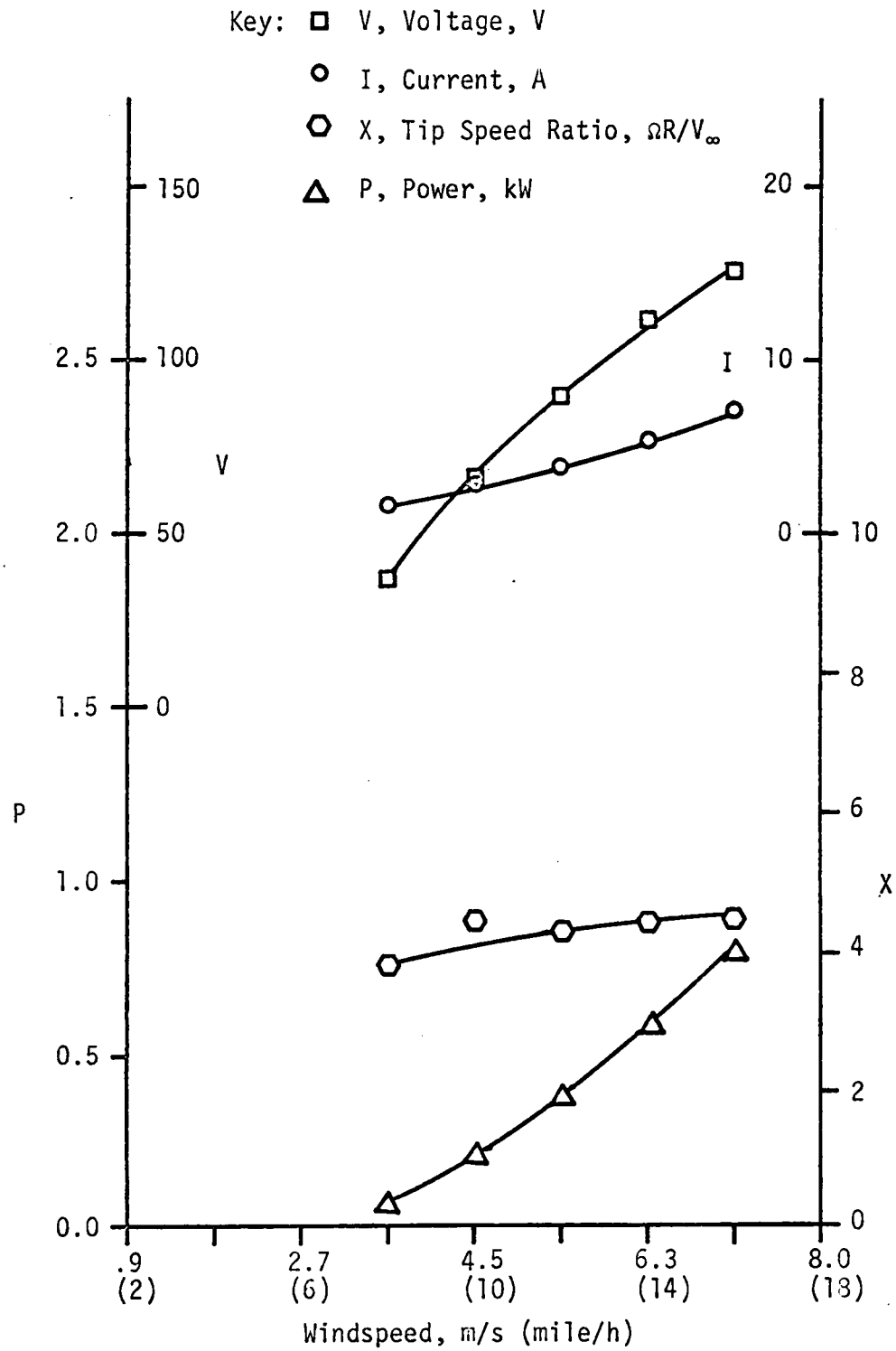

Figure 22. Performance Data, Case 3.

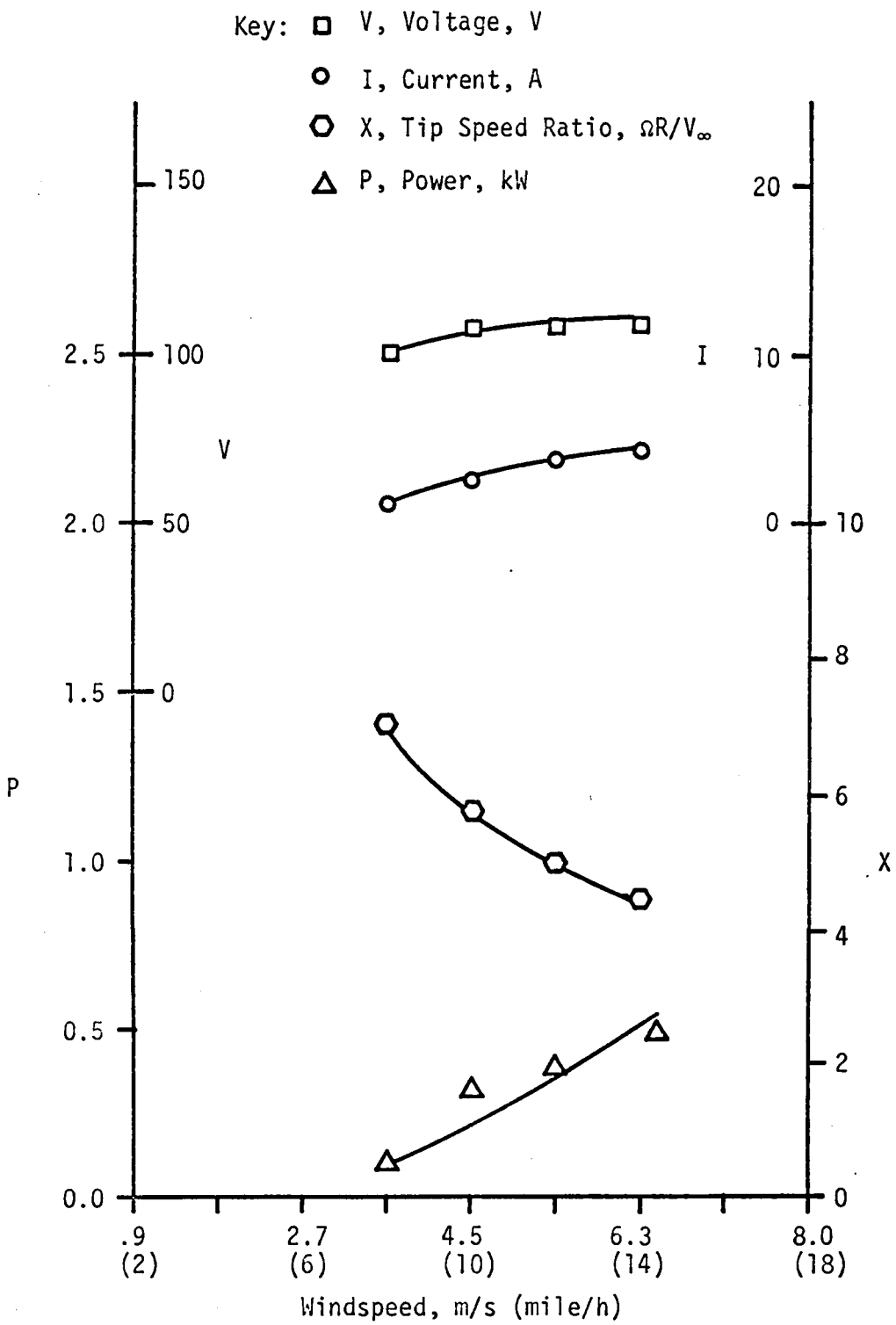

Figure 23. Performance Data, Case 4.

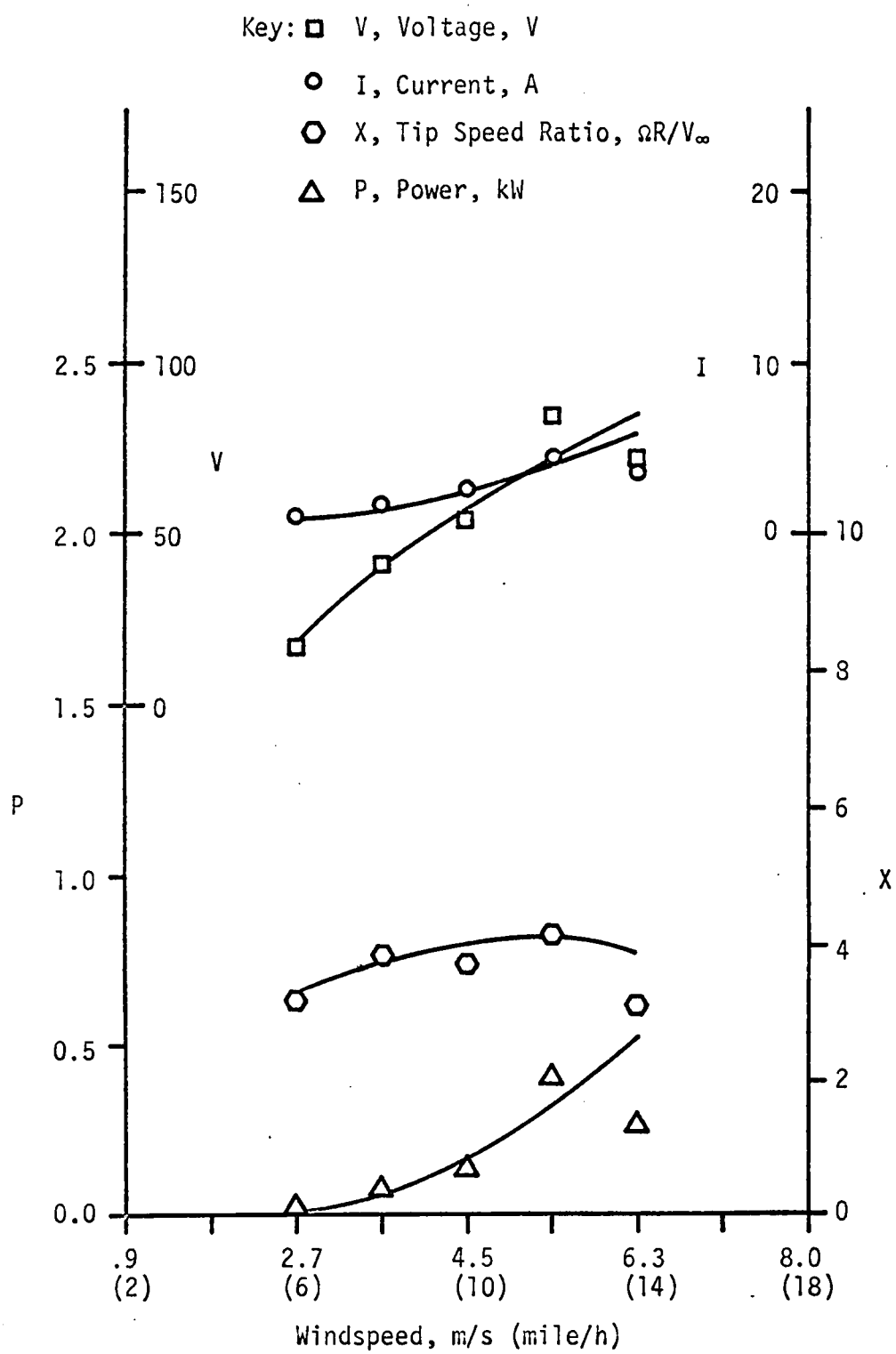

Figure 24. Performance Data, Case 5.

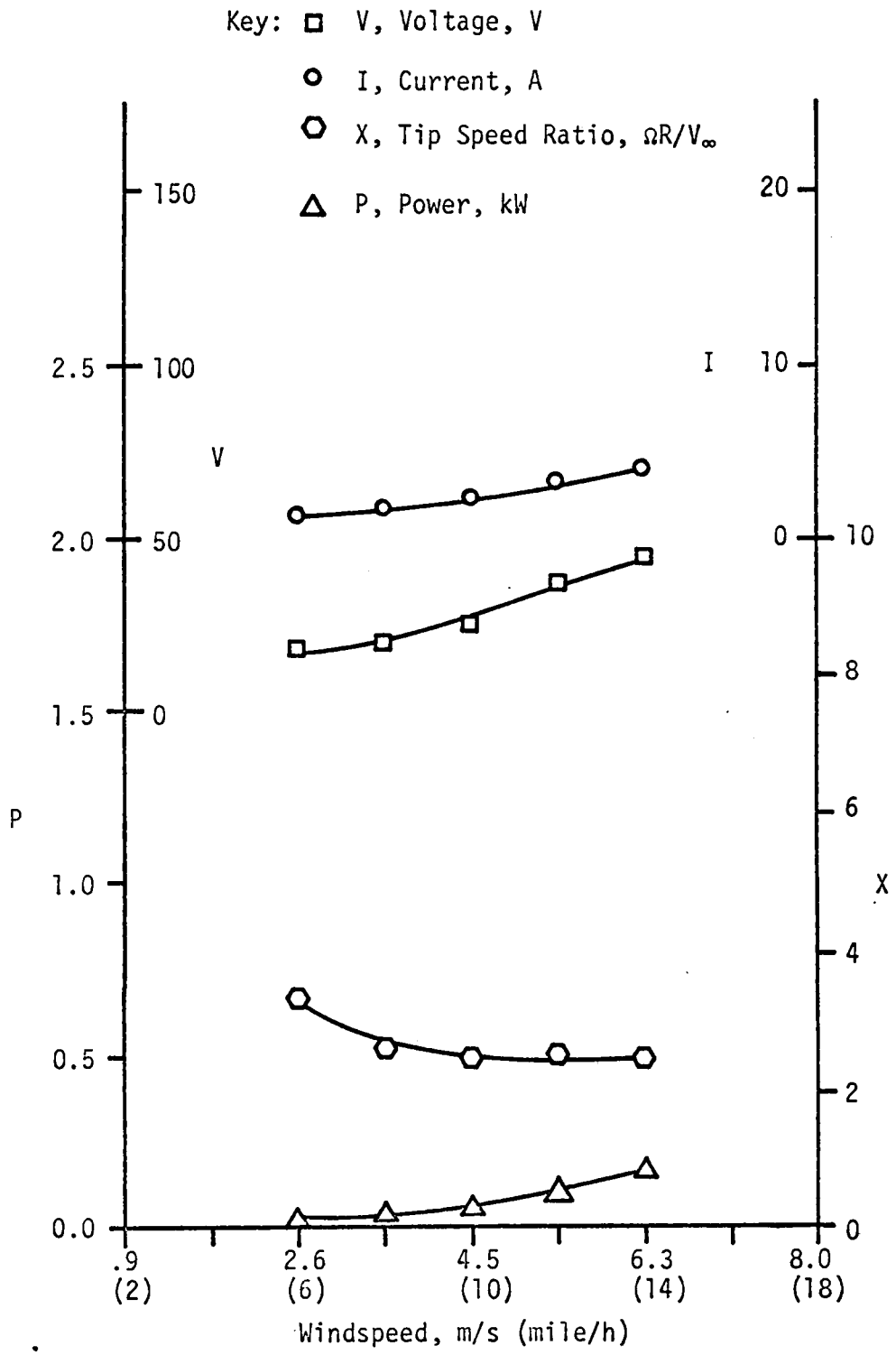

Figure 25. Performance Data, Case 6.

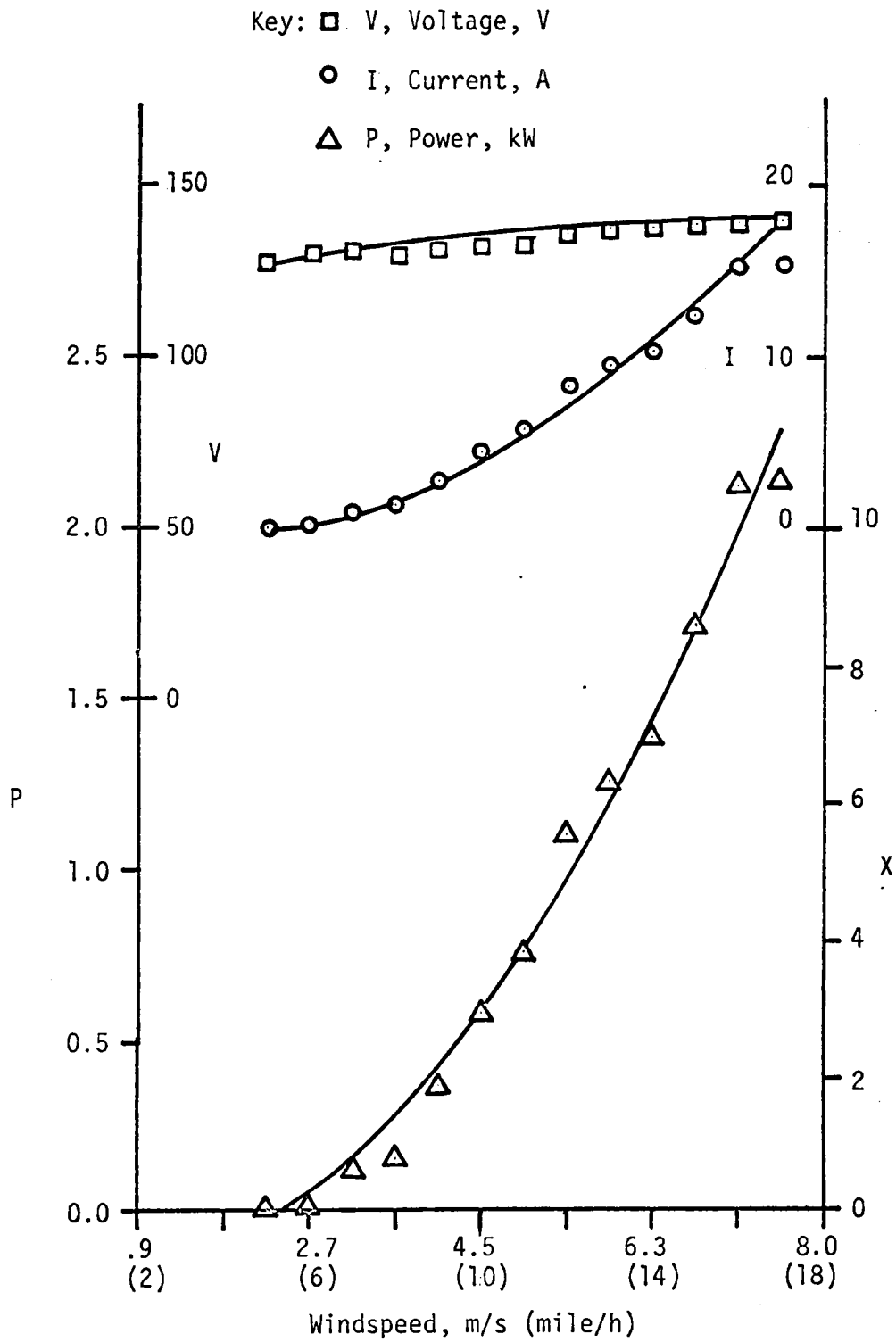

Figure 26. Performance Data, Case 7.

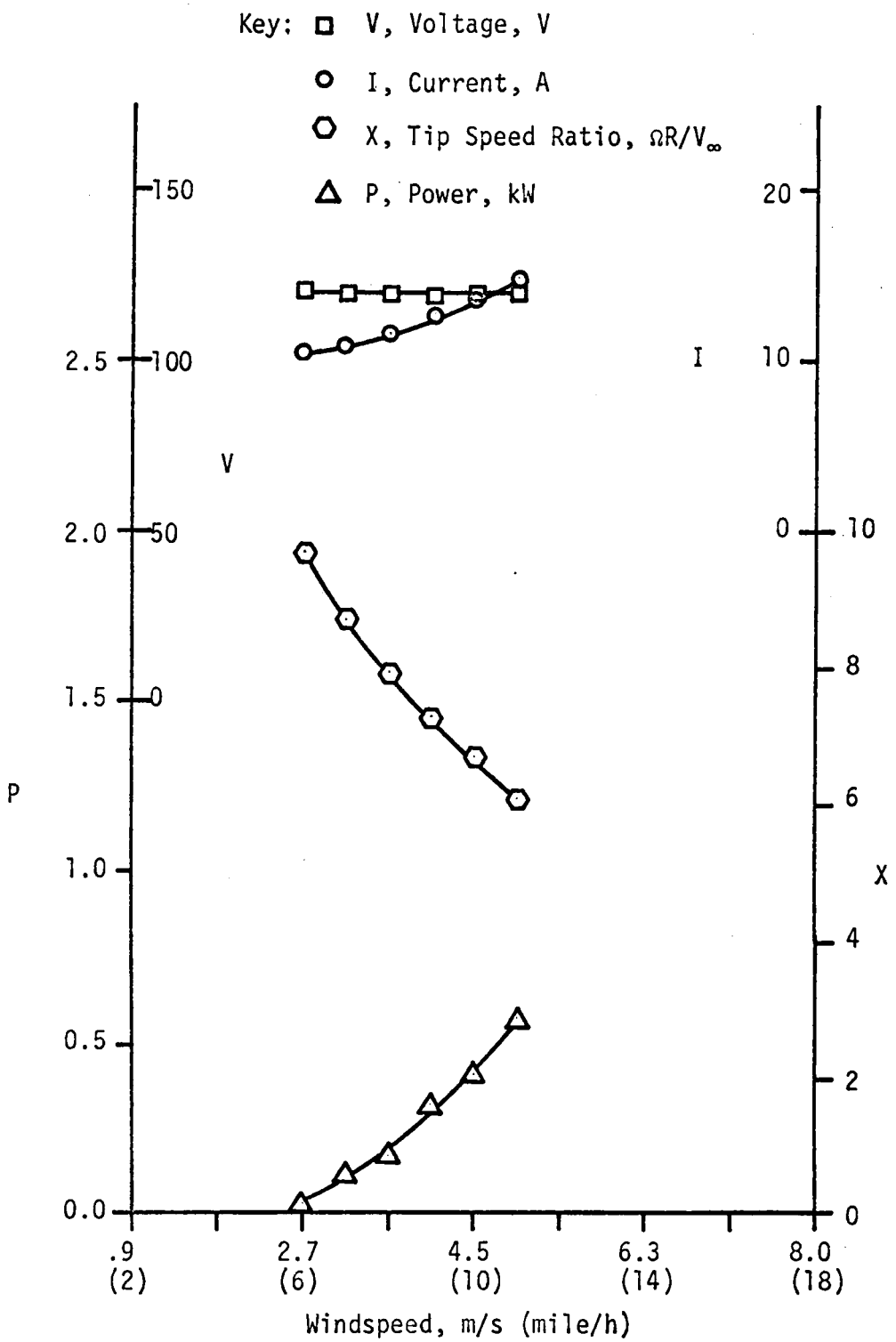

Figure 27. Performance Data, Case 8.

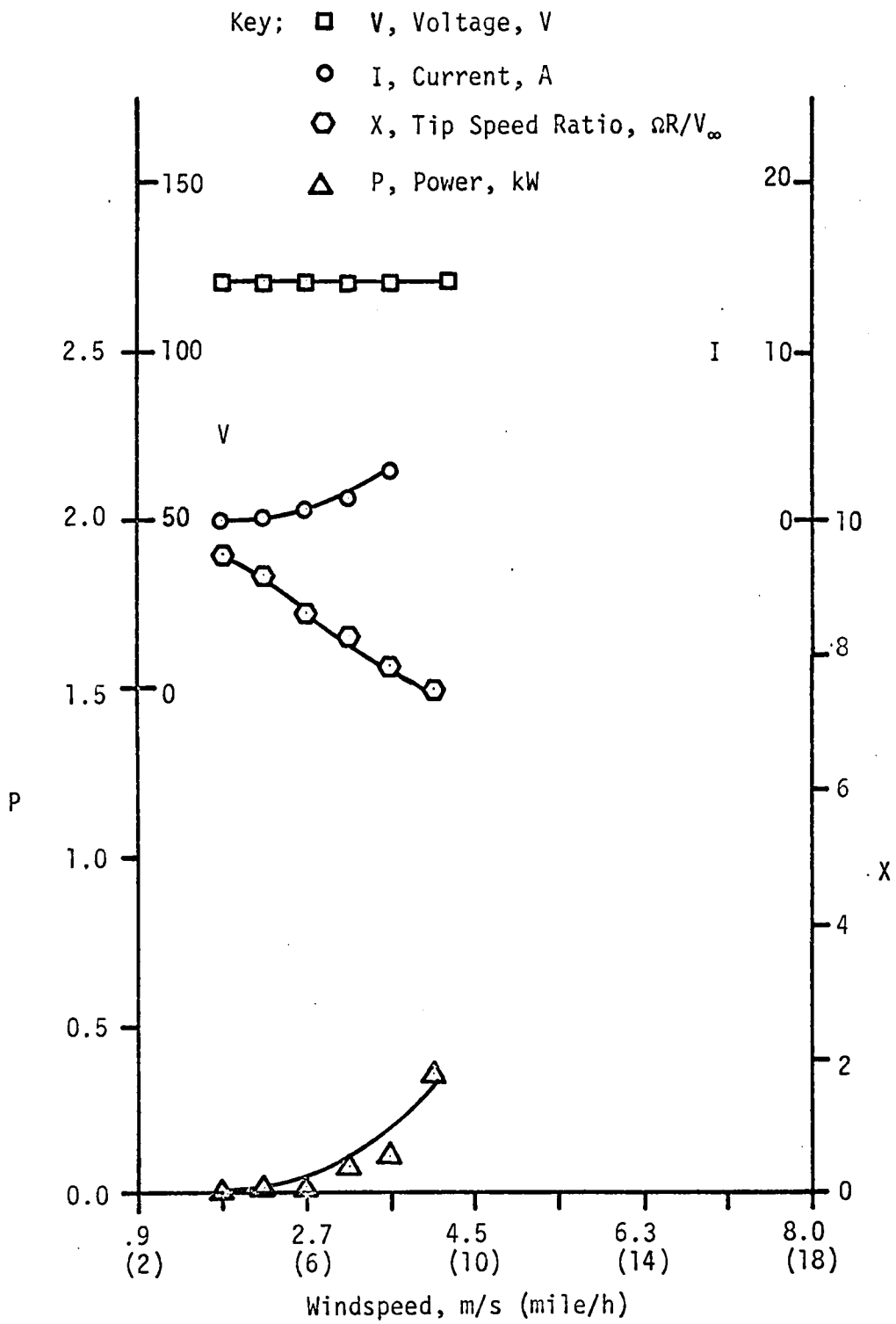

Figure 28. Performance Data, Case 9.

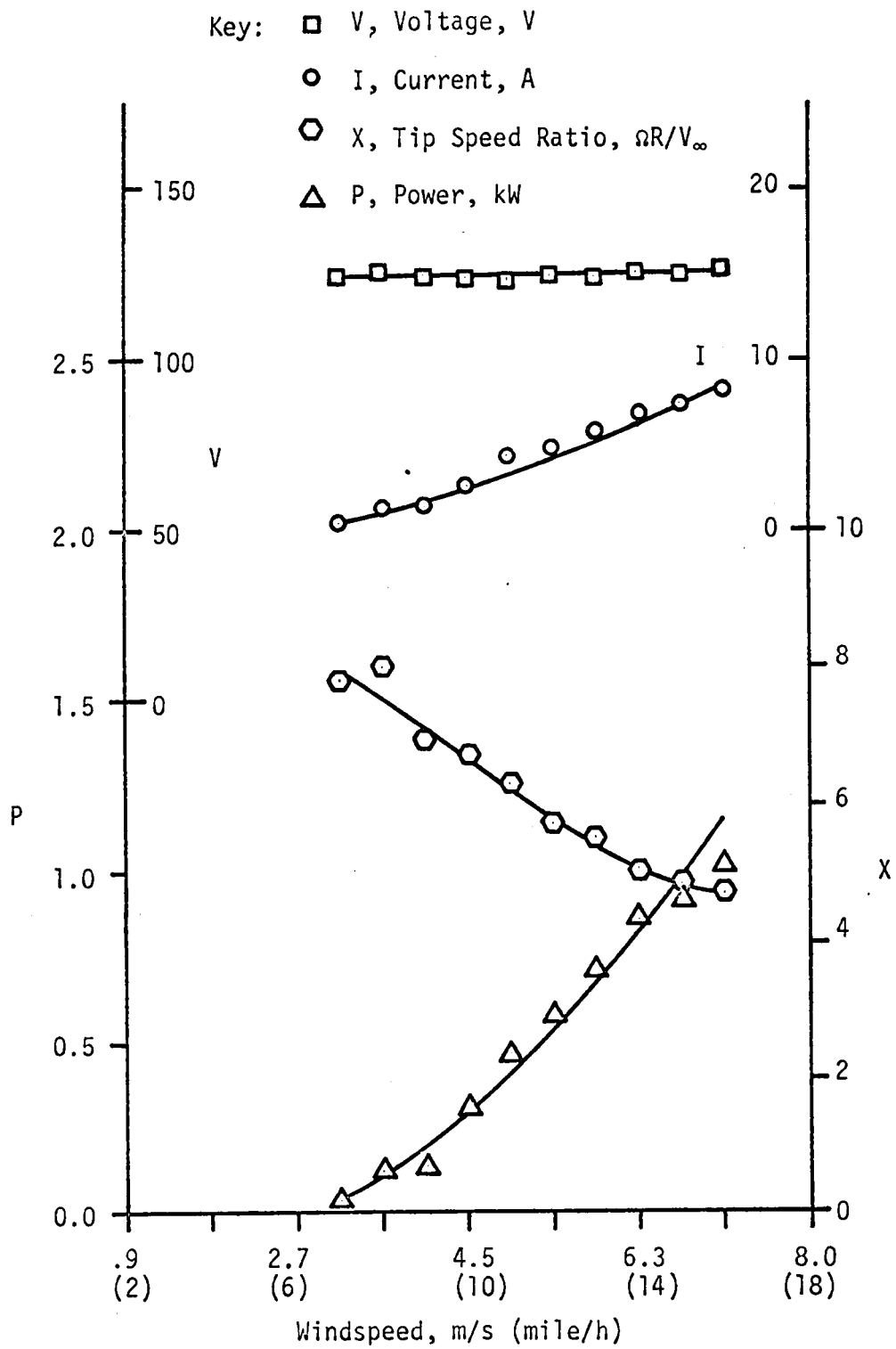

Figure 29. Performance Data, Case 10.

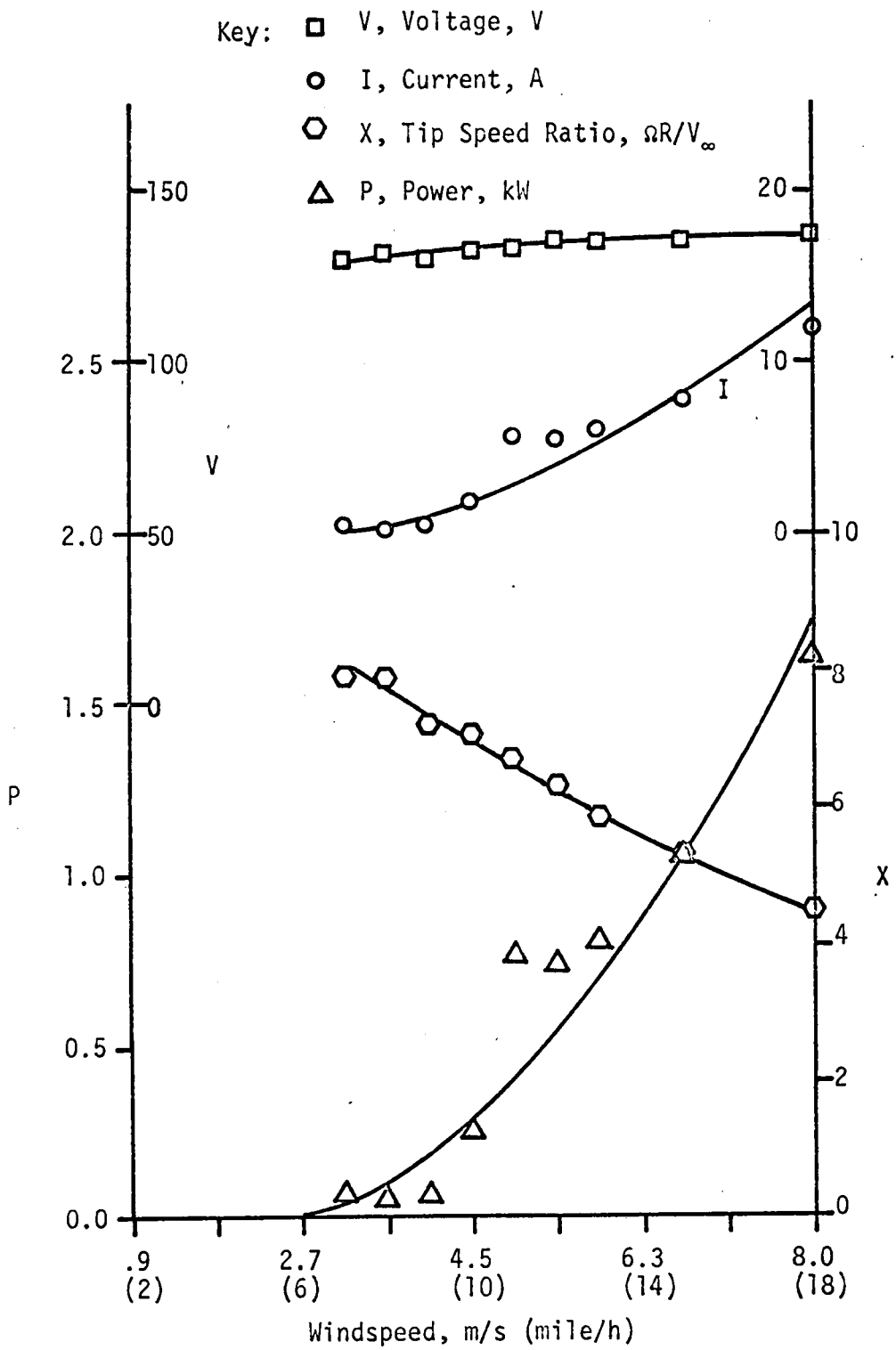

Figure 30. Performance Data, Case 11.

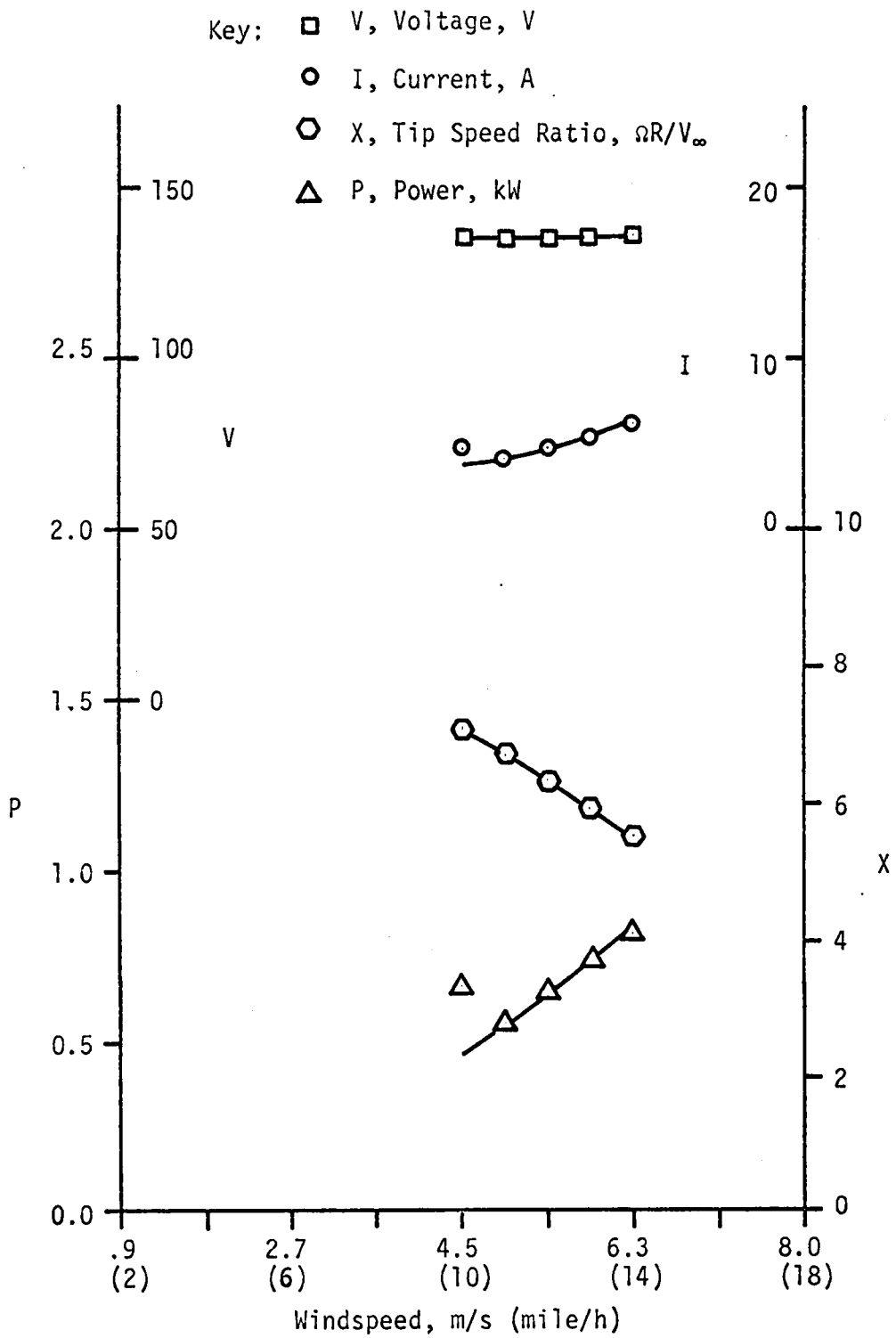

Figure 31. Performance Data, Case 12.

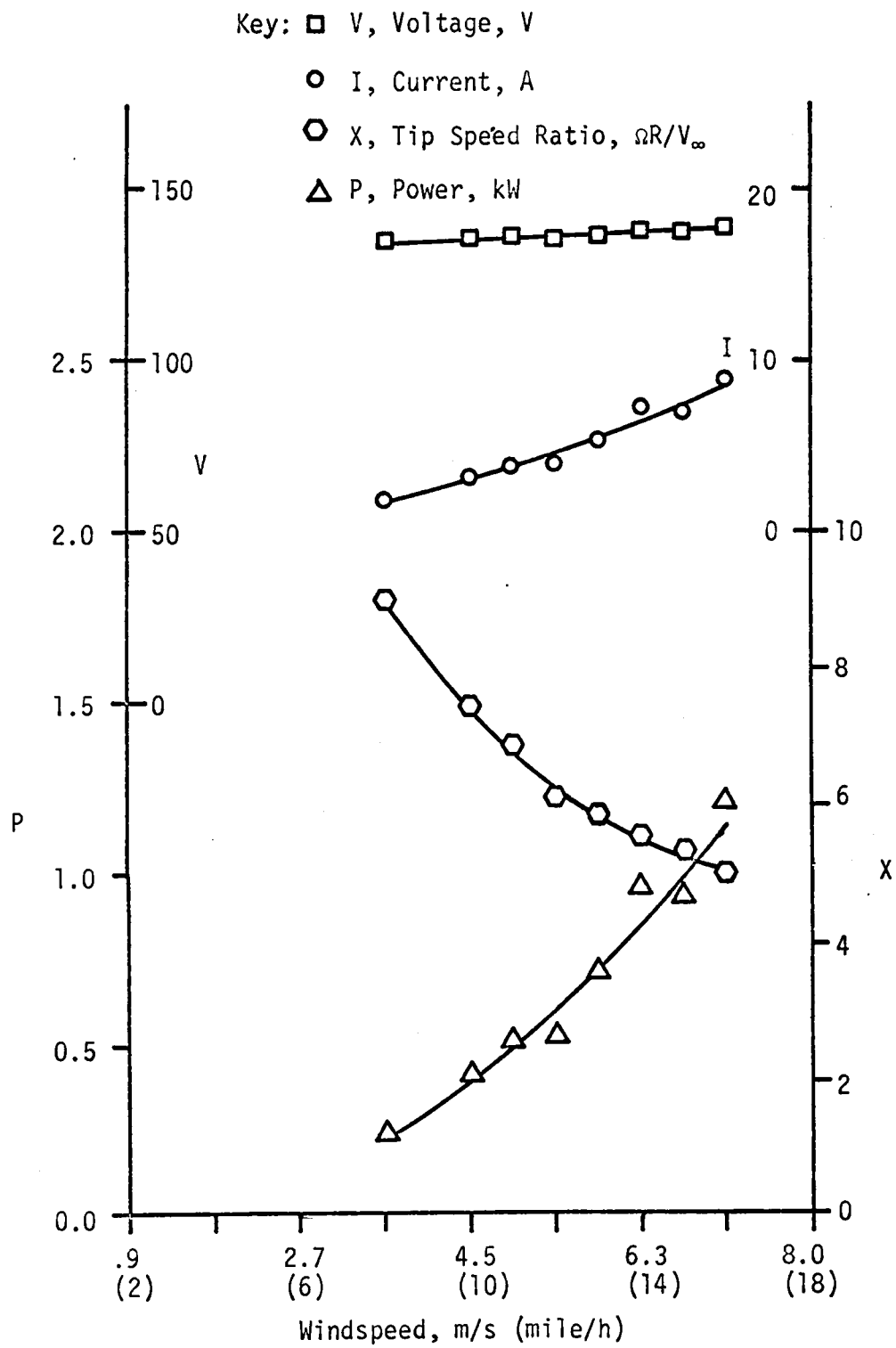

Figure 32. Performance Data, Case 13.

XI. DISCUSSION

Interpretation of Data

Figures 33 and 34 are mean power curves vs. wind for the resistive load tests and the battery load tests respectively. The ideal power curve is also plotted for reference.

The first observation that one can make after examining the data is that the windmill extracts more power from the wind when connected to the battery bank than when directly powering the resistive load. The second observation is that the windmill operates at higher tip speed ratios when used with a battery load. The reason for this is that when the alternator voltage falls below the battery voltage, the alternator is unloaded and the windmill is "free-wheeling". This is evidenced by the fact that the tip speed ratio is high at low wind speeds and decreases as enough voltage is generated to charge the batteries. The tip speed ratio for the resistive load tests does not have a consistent identifying characteristic.

Table 4 lists the mean power output, power coefficient, and tip speed ratio for the resistive loads and the battery load, for each observed wind speed. Note that values of $\bar{C}_p$ above 0.20 correspond to tip speed ratios of between 6.1 and 7.2. This observation confirms the importance of maintaining the windmill blades at a good angle of attack. However, even the highest value of C_p obtained corresponds to an efficiency of only 39 per cent.

Manufacturer's data was not supplied for the WVG-120G wind turbine and comparison with Fig. B-1 is not possible as most of the data was

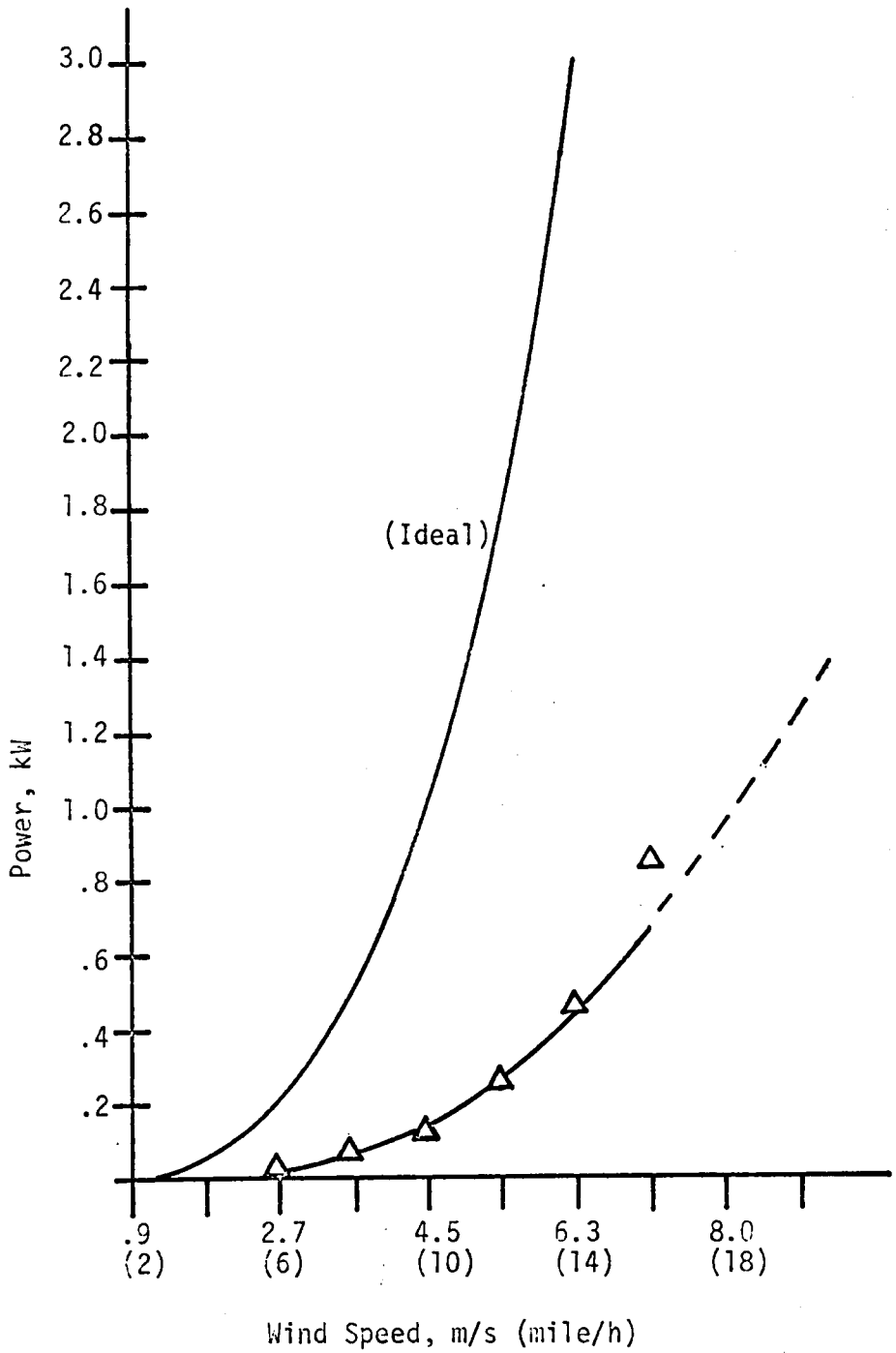

Figure 33. Mean Power Output Curve, Resistive Load.

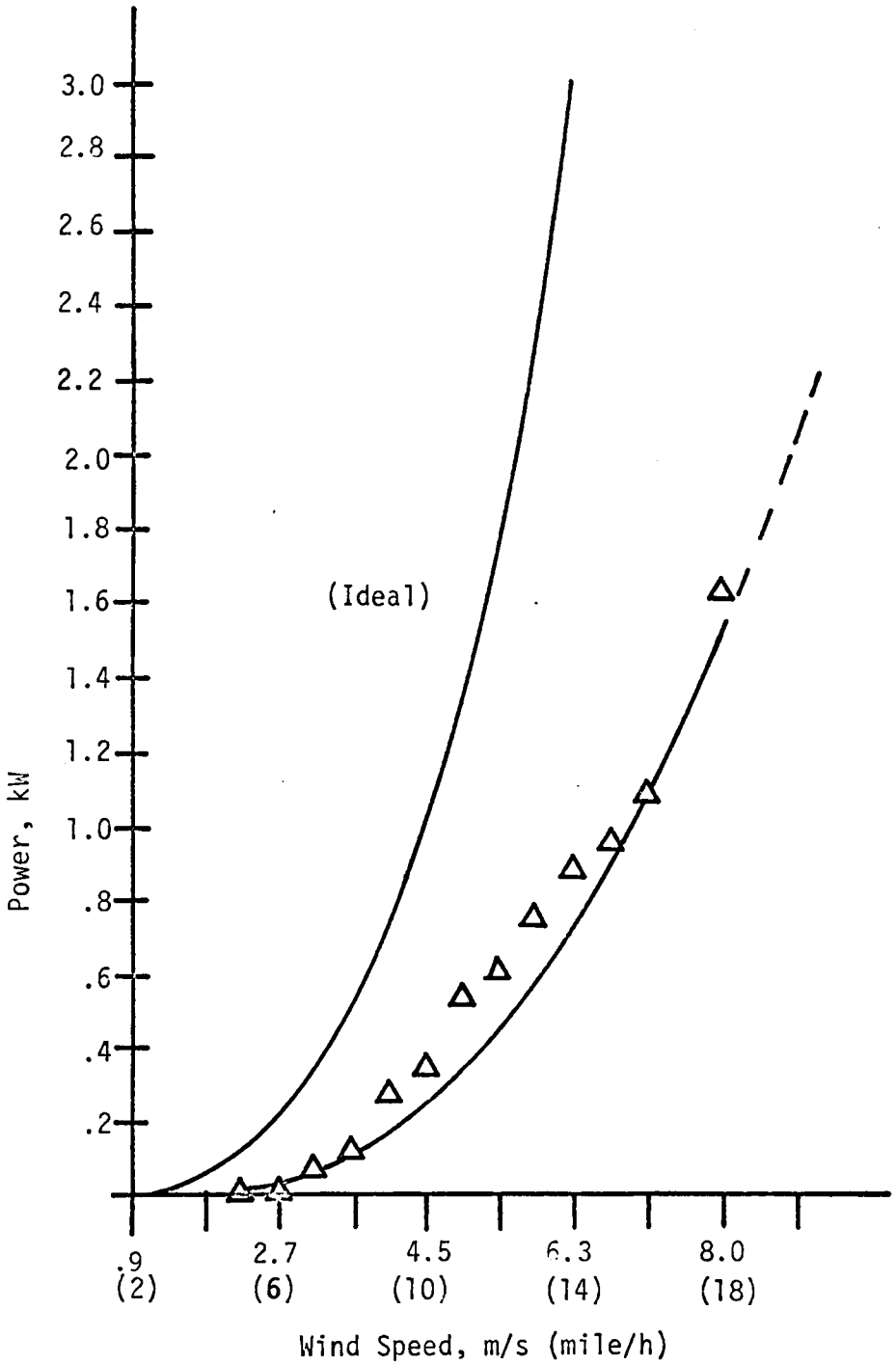

Figure 34. Mean Power Output Curve, Battery Load.

Table 4

Power Output Summary (Note)

V_∞		Battery Load				Resistive Load			
m/s	(mile/h)	$\bar{P}$ W	σ_p W	$\bar{C}_p$	$\bar{X}$	$\bar{P}$ kW	σ_p kW	$\bar{C}_p$	$\bar{X}$
2.2	(5)	9	0	0.05	9.2				
2.7	(6)	18	9	0.05	9.1	27	6	0.07	4.8
3.1	(7)	89	23	0.15	8.2				
3.6	(8)	131	46	0.15	8.1	73	25	0.09	4.7
4.0	(9)	271	89	0.22	7.2				
4.5	(10)	337	62	0.20	7.0	132	64	0.08	4.4
4.9	(11)	518	88	0.23	6.5				
5.4	(12)	579	47	0.20	6.1	258	120	0.09	4.7
5.8	(13)	726	39	0.19	5.7				
6.3	(14)	855	59	0.18	5.4	444	168	0.09	3.5
6.7	(15)	910	61	0.16	5.1				
7.2	(16)	1026	100	0.14	4.9	842	-	0.12	4.1
7.6	(17)								
8.0	(18)	1562	-	0.16	4.5				

NOTE: $\bar{P}$ Average Power Output

σ_p Standard Deviation of Power

$\bar{C}_p$ Average Power Coefficient

$\bar{X}$ Average Tip Speed Ratio

Values of $\bar{P}$, σ_p, and $\bar{C}_p$ are adjusted using the correction factor of 0.95 calculated in Appendix F.

obtained with the rotor running below 100 RPM. Because of the lack of comparative data it is necessary to make some assumptions concerning the cause of the low efficiency. If the gear train and alternator are assumed to have a combined efficiency of 0.70, and if miscellaneous system losses are assumed to be no greater than 0.10, the aerodynamic efficiency must be only approximately 0.62. This may be due to the poor profile (Fig. 8) which could lead to early separation and stall. The even lower efficiency obtained with the resistive load is thought to be due to the resistive load preventing the system from reaching optimum rotational speed (average tip speed ratio for resistive load was 4.4), causing most of the blade to be at a high angle of attack (Fig. 10). In gusty conditions it was noticed that the resistive load tended to brake the rotor during lulls and that during a gust the rotor had to be accelerated to operating speed. The unloading effect of a battery load helps to maintain a higher and more uniform rotor speed.

Load Switching and Sizing

A wind turbine system that could efficiently power a resistive load bank would be ideal to use as supplementary heating. It is believed that reducing the incremental load size to 1/15 the rated capacity would allow the windmill to operate with an effective tip speed ratio. It is envisioned that a load segmented at 1/15, 2/15, 4/15, 8/15 could be switched easily employing a comparator circuit with a binary output using only 4 switching SCR's. Such a circuit

would be much more effective than the 3-level switching now employed. The cost of semi-conductor switching vs. the relays and contactors of the Electro system is estimated to be much lower.

Battery or Direct Load

Although these tests show that a battery load allows the wind turbine to operate with higher efficiency, it must be remembered that only 54 - 60 per cent of the energy put into the battery will be recovered. This fact makes the overall performance of the resistive load comparable to that of the batteries. Thus it would appear that for optimum performance some sort of composite system is necessary. Power from the windmill would be directly used by the system, while a small battery bank would be used to store excess energy that the electrical system cannot use, and would be a reserve used during motor starting and in calm periods. A control system to accomplish this is being designed for use with the WVG-120G and the refrigeration system described by Blanton [13].

Power Multiplier Integrator

Although the cause of the inaccuracy of the power multiplier circuit was not discovered before the system was moved, it is believed that the idea is a sound one and should be explored further to enable automatic power recording. Integrated circuit devices are available which can replace all the functions used on the analog computer and the voltage controlled generator.

XII. CONCLUSIONS

1. Power produced by the Electro WVG-120G wind generator was measured for wind speeds in the range of 2 - 8 m/s (4 - 18 mile/h), using both a resistive load and a battery load. Output power varied from 0 to 1.6 kW for these wind speeds.

2. The power output using the resistive loads varied about 37 per cent for a given wind speed, showing the dependence of performance on load sizing and switching. By comparison, using the battery load, measured power output varied only about 20 per cent at a given wind speed.

3. The power coefficient varied from 0.05 to 0.23, and appeared to be dependent on the tip speed ratio. The highest value of C_p was obtained at a tip speed ratio of 6.5.

XIII. RECOMMENDATIONS FOR FURTHER RESEARCH

1. Conduct further performance evaluation at wind speeds of 7-18 m/s (15 - 40 mile/h).
2. Investigate all means to optimally "tune" the wind turbine:

   Calibrate the alternator in a test rig.

   Dynamically balance the rotor.

   Improve the airfoil and twist of the blades.
3. The use of a data logger is recommended to enable more precise measurements, along with the capability of direct transfer of data to the VPI&SU computer system.
4. Develop a better switching system for direct heating.
5. Develop on-rotor instrumentation to measure air pressures and blade stresses.

XIV. LITERATURE CITED

1. Schetz, J. A., W. O'Brien, H. Moses, T. Weishaar, and D. Vaughan, Application of Windmills to Apple Cooling and Storage, Progress Report for the Period November 1976 - February 1977, Virginia Polytechnic Institute and State University, 1977.

2. Putnam, Palmer Cosslett, Power From the Wind, Van Nostrand Reinhold Company, New York, 1948.

3. Walter, Samuel, "Briefing the Record", Mechanical Engineering, August 1977, p. 45.

4. Westh, H. Claudi, "A Comparison of Wind Turbine Generators", Proceedings of the Second Workshop on Wind Energy Conversion Systems, Washington, D.C., 1975.

5. Rueth, Nancy, "Energyscope", Mechanical Engineering, August 1977, p. 19.

6. Liljedahl, L. A., "Wind Energy Use in Rural and Remote Areas", Proceedings of the Second Workshop on Wind Energy Conversion Systems, Washington, D.C., 1975.

7. Wilson, R. E., "Applied Aerodynamics of Wind Power Machines", Proceedings of the Second Workshop on Wind Energy Conversion Systems, Washington, D.C., 1975.

8. Wilson, R. E., and P. B. S. Lissaman, Applied Aerodynamics of Wind Power Machines, Oregon State University, Corvallis, Or., 1974.

9. Oman, R. A., and K. M. Foreman, "Cost Effective Diffuser Augmentation of Wind Turbine Power Generators", Proceedings of the Second Workshop on Wind Energy Conversion Systems, Washington, D.C., 1975.

10. Smulders, P. T., "Physical Aspects of Windmill Design", Physics in Technology, September, 1976.

11. Zlotnik, M., "Energy Storage for Wind Energy Conversion Systems", Proceedings of the Second Workshop on Wind Energy Conversion Systems, Washington, D.C., 1975.

12. Blanton, J. C., "Design of a Wind - Powered Cooling System for an Apple Storage Facility", M.S. Thesis, Virginia Polytechnic Institute and State University, 1977.

13. Weick, F. E., Aircraft Propeller Design, McGraw-Hill, New York, 1930.

14. Electro, GmbH, Operating Manual for WVG-120G, Winterhur, Switzerland.

15. Holman, J. P., Experimental Methods for Engineers, McGraw-Hill, New York, 1971.

XV. APPENDICES

Appendix A

Specifications of Electro WVG-120G

Table A-1

Specifications of Electro

WVG-120G Wind Generator

Rated Output	10 kW
Output Voltage	110 V (3-Phase A. C.)
Frequency Range	50-130 Hz
Propeller Speed Range	100 - 250 RPM
Number of Propeller Blades	3
Field Regulation	Combination of 2 permanent magnets and 2 field rotor sections
Field Current	1.2 - 1.5 A
Field Voltage	50 - 80 V
Generator Weight	2795 N (628 LBF)

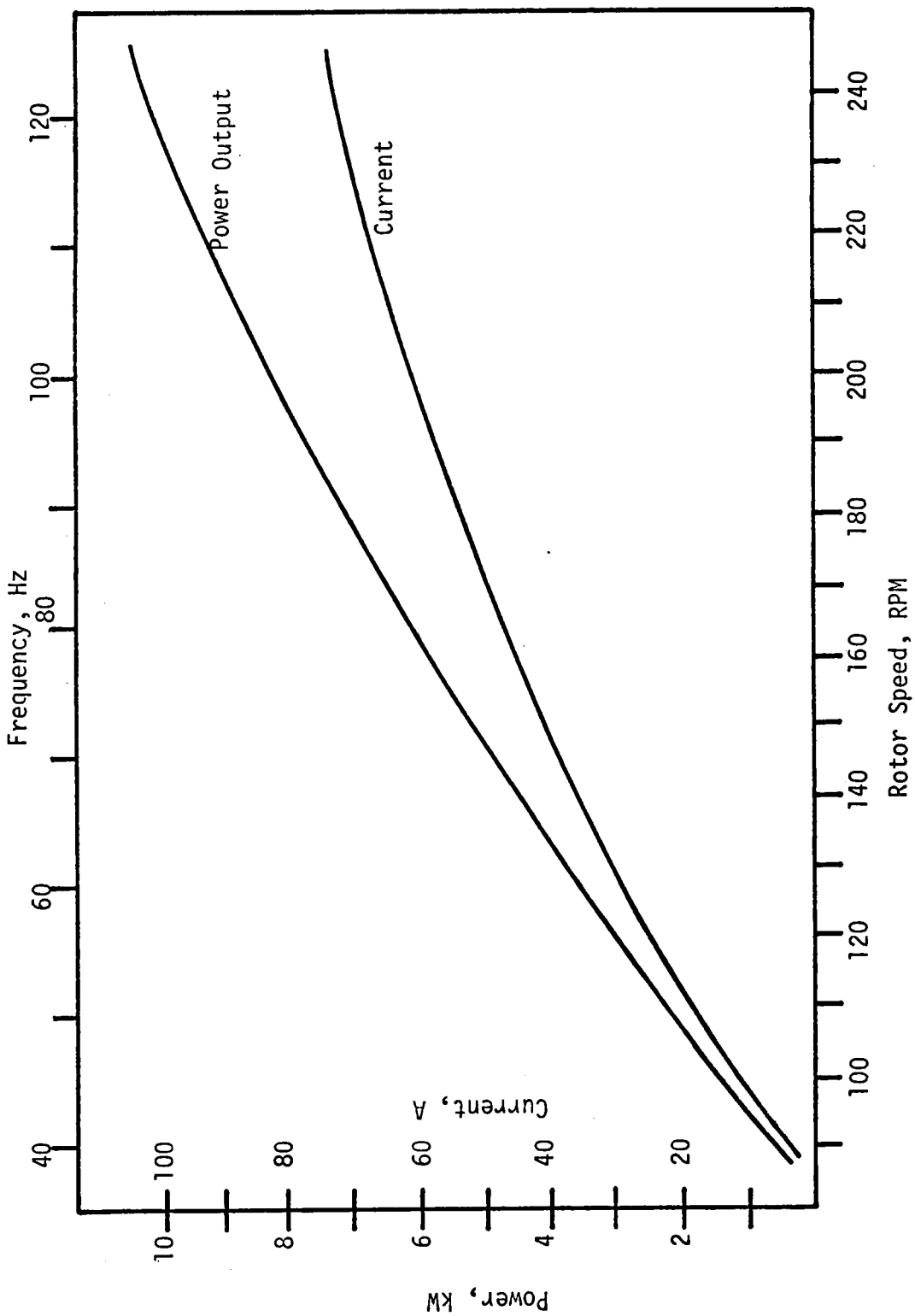

Figure A1. Generator Characteristics. (From Reference 14)

Appendix B

Electrical Schematics of Electro WVG-120G

Table B-1

Electrical Schematic Legend

SAB	Control Switch Limiter
SSp	Voltage Limiter
c	Spark Discharge Capacitor
R	Resistors
SpKP	Voltage Control Potentiometer
ES	Limit Switch for Brake
SM	Control Motor
Sch	Collector Ring
VMS	Voltmeter Switch
Si	Main Fuse
V	Voltmeter
A	Ammeter
MK	Ground Terminal
o	Insulated Terminal
I	Diode Switch for 10 - 40 V
II	Diode Switch for 40 - 120 V
3	Current Carrying Lead for Automatic Control
4	Wind Pressure Switch Lead
8	Starting Circuit Lead
SJB	Starting Relay
d1,d2	Relay type MK2, 24 V DC
c1,c2	Load Contactor

A	Load Carrying Lead
B	Contactor Switching Relay Lead
C_A	Contactor Switching Relay Capacitor
R,S,T	3-Phase Leads
F	Field Winding
ZL	Zener Diode Switch

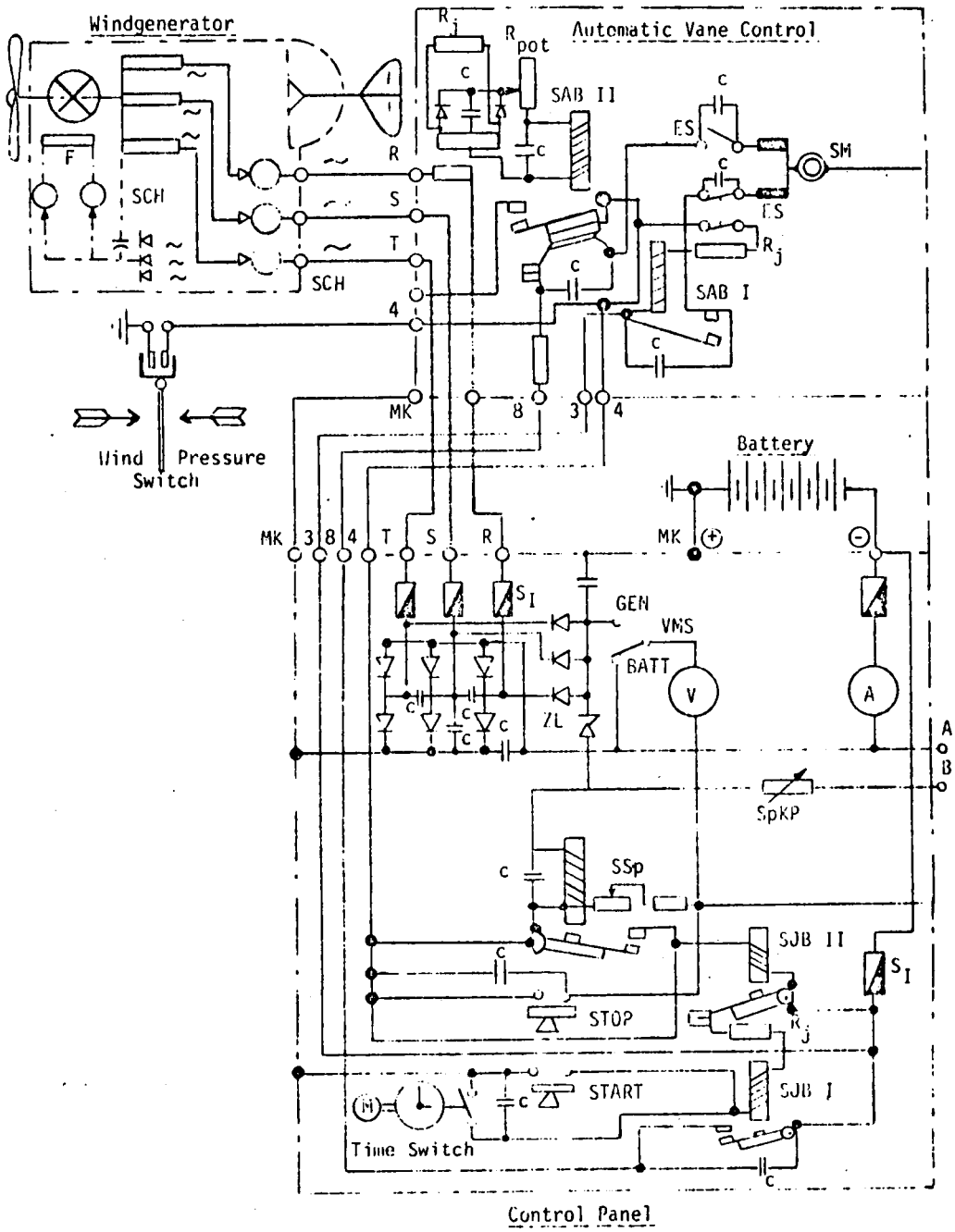

Figure B1. WVG-120G Control Circuit.
(From Reference 14)

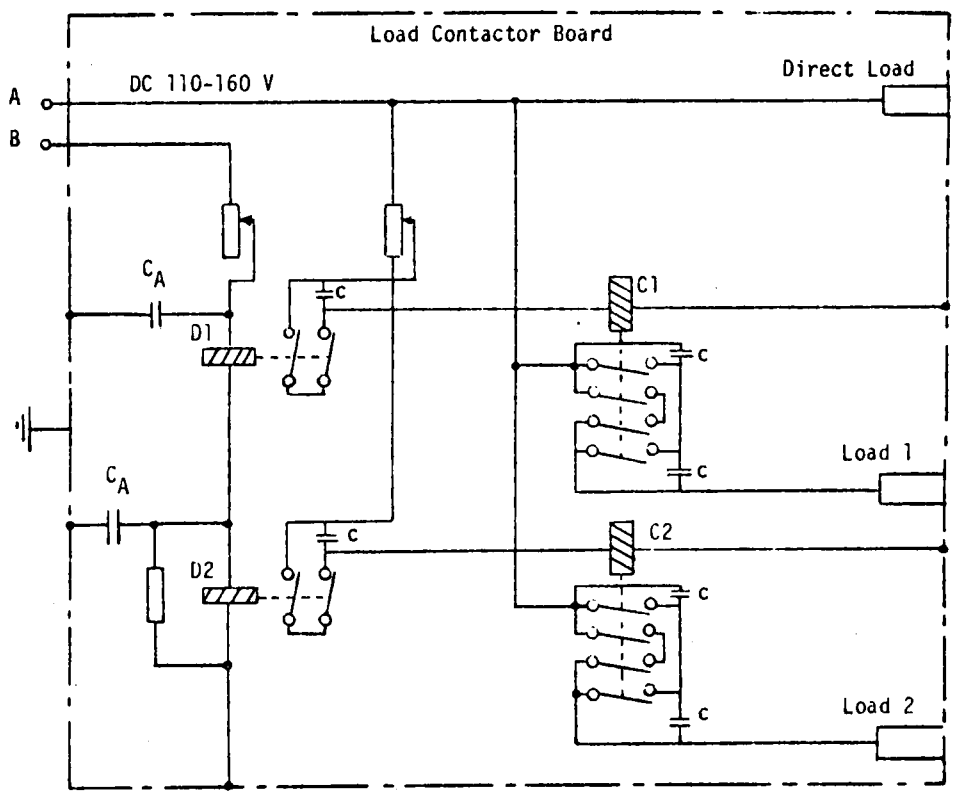

Figure B2. WVG-120G Load Contactor Board.
(From Reference 14)

Appendix C

Resistive Load Calibration Data

Table C-1

1000 W Resistive Elements

Voltage (V)	Current (A)									
	DL-1	DL-2	L1-1	L1-2	L1-3	L2-1	L2-2	L2-3	L2-4	L2-5
25	0.9	1.0	1.0	1.0	1.0	1.0	1.0	1.0	1.0	1.0
50	1.9	1.9	1.9	1.9	1.9	2.0	2.0	1.9	2.0	2.0
75	2.8	2.9	2.9	2.9	2.9	2.9	3.0	2.9	2.9	2.9
100	3.7	3.8	3.8	3.8	3.7	3.8	3.8	3.7	3.8	3.7
125	4.6	4.7	4.7	4.7	4.7	4.7	4.8	4.7	4.7	4.7
150	5.5	5.6	5.6	5.6	5.6	5.6	5.6	5.6	5.6	5.6

Table C-2

Alternate Resistive Elements

100 W Elements		600 W Elements	
Voltage (V)	Current (A)	Voltage (V)	Current (A)
25	0.2	25	0.6
50	0.3	50	1.3
75	0.37	75	1.9
100	0.45	100	2.6
125	0.5	125	3.2
150	0.6	150	3.8

Note: 100 W elements used in DL-2 in test case 1, 2, 4, and 5.

Appendix D

Specifications of Modified Nife C3600 Battery

Table D-1

Specifications of Modified Nife C3600 Battery

Manufacturer: Nife Incorporated

Model Number: C3600

Cell Type: KB-12 Nickel Cadmium

Open Circuit Voltage: 1.33 - 1.35 V/Cell

Number of Cells: 91 in series

Rated Capacity: 123 A-h

Discharge Specifications:

- Normal Rate 30A
- Normal Time 4 h
- Initial Voltage 1.3 V/Cell
- Average Voltage 1.2 V/Cell
- Final Voltage 1.0 V/Cell

Charge Specifications:

- Maximum Constant Current Rate 34.6 A
- Time at Maximum Rate 5 h
- Voltage at Maximum Rate 1.40 - 1.72 V/Cell
- Maximum Constant Voltage Rate 1.55 V/Cell
- Float Voltage (Trickle Charge) 1.42 V/Cell

Appendix E

Measurement System Calibration Data

Table E-1

Voltmeter Calibration Data

Instrument: Veritas V-925 VOM

Date: August 9, 1977

Conducted by: W. F. O'Brien, Jr.

Standard: Twinco Calibrator

Voltage Actual (V)	Voltage Indicated (V)
0-25 V DC	
5.0	5
10.0	9.8
15.0	14.7
20.0	19.5
25.0	24.8
0-100 V DC	
10	11
30	30
50	49.5
100	100
0-500 V DC	
100	100
200	195
500	495

Table E-2

Ammeter Calibration Data

Instrument: Weston Model 430 Ammeter, Serial No. 19991

Date: August 9, 1977

Conducted by: W. F. O'Brien, Jr.

Standard: Twinco Calibrator

Current Actual (A)	Current Indicated (A)
0-10 A DC	
0.0	0.03
2.0	2.0
5.0	5.0
10.0	10.0

Table E-3

Electrical Measurement System Calibration Data (Note)

Instrument: Voltage Divider Circuit

Current Shunt

Hewlett Packard Model 4100 B Recorder

EAI TR-20 Analog Computer

Data: August 25, 1977

Conducted by: T. E. Benim

Standard: Veritas V-925 VOM

Weston Model 430 Ammeter

Actual Voltage (V)	Actual Current (A)	Actual Power (kW)	Recorded Voltage (V)	Recorded Current (A)	Recorded Power (kW) (Calculated)	TR-20 Displayed Power (kW)
0	0.0	0.0	0	0.0	0.0	0.0
25	0.9	0.023	25	1.0	0.025	0.0
50	1.9	0.095	50	2.0	0.100	0.0
75	2.8	0.210	73	3.0	0.220	0.24
100	3.7	0.370	97	4.0	0.388	0.64
125	4.5	0.563	121	4.9	0.593	1.2
150	5.4	0.810	145	5.9	0.855	1.7
0	0.0	0.0	0	0.0	0.0	0.0
25	2.0	0.050	25	2.1	0.053	0.0
50	3.8	0.190	49	4.1	0.201	0.24
75	5.7	0.427	73	6.2	0.453	0.86
100	7.5	0.750	96	8.0	0.768	1.7
125	9.3	1.16	120	10.0	1.20	2.4
150	11.0	1.65	144	12.0	1.73	3.4

Note: Calibration performed using a DC power supply to simulate windmill output.

Actual Voltage (V)	Actual Current (A)	Actual Power (kW)	Recorded Voltage (V)	Recorded Current (A)	Recorded Power (kW) (Calculated)	TR-20 Displayed Power (kW)
0	0.0	0.0	0	0.0	0.0	0.0
25	3.0	0.075	25	3.2	0.080	0.0
50	5.8	0.290	49	6.2	0.304	0.65
75	8.6	0.645	72	9.3	0.670	1.6
100	11.3	1.130	95	12.0	1.14	2.3
125	13.8	2.07	119	15.0	2.23	3.6
150	16.5	2.47	144	18.0	2.59	5.2
0	0.0	0.0	0	0.0	0.0	0.0
25	4.0	0.100	25	4.2	0.105	0.1
50	7.9	0.395	48	8.5	0.408	1.0
75	11.5	0.863	73	12.5	0.912	1.8
100	15.0	1.50	96	16.3	1.57	2.9
125	18.3	2.29	120	20.0	2.40	5.0
0	0.0	0.0	0	0.0	0.0	0.0
25	5.0	0.125	24	5.4	0.130	0.25
50	9.6	0.480	49	10.5	0.515	1.25
75	13.3	0.998	72	15.5	1.12	2.0
100	18.5	1.85	95	20.0	1.90	4.0

Appendix F

Uncertainty Analysis

Uncertainty Analysis

All instruments used in this thesis were calibrated or checked for accuracy except for the oscilloscope and its time base which were used as a reference in calibrating the F/V converter, and the Beckman counter. The results of the electrical measurement system calibrations are tabulated in Appendix E. The results of tests on the other instruments are discussed below.

The F/V system failed before a documented calibration could be performed but a preliminary operational check using the VCG as a signal and the oscilloscope as a reference showed the accuracy to be within $\pm$ 0.02%. Similarly the frequency counter was accurate to within $\pm$ 1 digit ($\pm$ 1 Hz).

The Stewart anemometers were checked in the VPI&SU open throat wind tunnel and were found to be accurate within $\pm$ 1 digit. For a 1 minute average this corresponds to $\pm$ 0.5 m/sec ($\pm$ 1 mile/h). Tests with two recently purchased Stewart anemometers show that they indicate about 1.3 - 1.8 m/s (3-4 mile/h) low in the range from 6.7 - 17.9 m/sec (15 - 40 mile/h). However these tests were run in a different wind tunnel and wind speeds below 6.7 m/sec (15 mile/h) could not be obtained. It is recommended that all anemometers used in this project be calibrated under identical conditions to obtain consistent calibration data. It was decided to assign an uncertainty to the Stewart anemometers of $\pm$ .5 m/sec (1 mile/h) or $\pm$ 10%, whichever is greater.

Correction factors and uncertainties were calculated using the mean value of reading/actual values and the standard deviation of these values. The results are:

VOM	1.00 ± 0.03
Ammeter	1.00 ± 0.03
Voltage Recorder	1.03 ± 0.02 (Based on VOM)
Current Recorder	0.93 ± 0.02 (Based on Ammeter)
TR-20 Computed Power	0.59 ± 0.81 (Based on VOM + Voltmeter)

Since the voltage and current recorders were calibrated using a secondary source, the precision of these recorders was estimated using a sum of squares technique outlined by Holman [15]. The uncertainty of both the voltage measurement and the current measurement are equal to:

$$W_I = W_V = \pm[(W_{meter})^2 + (W_{recorder})^2]^{1/2}$$

$$= \pm[(0.03)^2 + (0.02)^2]^{1/2}$$

$$= \pm 0.04$$

The power calculated from the values of recorded voltage and current was plotted and found to be linear, with true power equal to 0.95 times calculated power (0.93 x 1.03 = 0.95). The uncertainty is:

$$Wp = \pm[(W_V)^2 + (W_I)^2]^{1/2}$$

$$= \pm[(0.04)^2 + (0.04)^2]^{1/2}$$

$$= \pm 0.06$$

Similarly, for tip speed ratio:

$$W_X = \pm[(W_f)^2 + (W_{V_\infty})^2]^{1/2}$$

$$W_X = \pm[(.02)^2 + (.1)^2]^{1/2}$$

$$W_X = \pm 0.1$$

and, for power coefficient:

$$W_{Cp} = \pm[(Wp)^2 + 3(W_{V_\infty})^2]^{1/2} = \pm 0.18$$

Appendix G

List of Equipment

Table G-1

List of Equipment

Ammeter: Weston Model 430

Analog Computer: EAI Model Tr-20

Anemometer: Belfort Model 5-349A Totalizing Anemometer

Stewart 1/60th Mile Anemometer

Counter: Beckman Universal EPUT Timer

Digital Panel Meter: Datel Model 2100 A

Frequency to Voltage Converter: Teledyne Philbrick Model 4702

Oscilloscope: Tektronix Type 564 Storage Oscilloscope

Tektronix Type 2A63 Differential Amplifier

Tektronix Type 2B67 Time Base

Recorder: Hewlett - Packard Model 7100 B Strip Chart Recorder

Mosely Model 7100 B Strip Chart Recorder

Belfort Model 6081 Event Recorder

Voltage Controlled Generator: Wavetek Model III

Voltmeter: Veritas V 925 VOM

The vita has been removed from the scanned document

PERFORMANCE MEASUREMENT OF A TEN KILOWATT HORIZONTAL AXIS WIND TURBINE

by

Thomas E. Benim

(ABSTRACT)

A system to measure the performance of a 10 kW horizontal axis wind turbine was designed and was employed to test an Electro WVG-120G wind generator.

Parameters measured were wind speed, voltage, current, and frequency. Output power and tip speed ratio were calculated from the measured parameters. A system to automatically calculate instantaneous power and to integrate power was developed. An improved digital anemometer odometer was designed and built.

Tests were performed with the windmill powering a resistive heating load as well as charging a battery.